MEASURING HUMAN DIAPHRAGM ELECTRICAL ACTIVITY: INFLUENCE OF BREATHING PATTERN AND END-INSPIRATORY LUNG VOLUME

by

FRANK NIRO

B.Sc. Honours Kinesiology, McGill University, 2019

B.Sc. Microbiology and Immunology, McGill University, 2012

A THESIS SUBMITTED TO McGILL UNIVERSITY IN PARTIAL FULFILLMENT OF THE REQUIREMENTS OF THE DEGREE OF MASTER OF SCIENCE

in

THE FACULTY OF EDUCATON
(Department of Kinesiology & Physical Education)

McGILL UNIVERSITY

MONTREAL, QUEBEC, CANADA

May 2020

TABLE OF CONTENTS

Figures & Tables

Acknowledgments

First and foremost, I'd like to thank my supervisor Dr. Dennis Jensen. I consider myself fortunate to have been directly trained and mentored by you over these past 4 years. From sitting down and outlining/drawing out our experiment, to being beside me on those long nights of pilot testing, helping me navigate the uncertainty of building a *de novo* experiment up to the analysis and writing; you have been there for me each step of the way. Sharing ideas, providing support and helping me persevere, I could not have done this without you. As I prepare to complete my graduate studies, I leave with a wealth of knowledge, new insights (both personally and professionally) which I will carry with me for the rest of my career. Thank you for welcoming me to CERPL, being my supervisor, my mentor, and a friend.

I'd also like to thank Benjamin Dubuc for his invaluable contribution in co-designing the experimental circuit, building the breathing trial matrix and many other aspects which made this study possible. I will always remember those 'pioneering months' with that 3L syringe, metronome and daily 'spirometry lung Olympics'. Thank you for your hard work, innovative acumen, and making this fun.

I would like to thank my committee members, Drs. Jean Bourbeau and Ben Smith, for their valuable insight and recommendations that helped improved our study. Jean, thank you for taking me under your wing and welcoming me to the Montreal Chest Institute's pulmonary rehab team, and for taking the time to be my clinical mentor and teaching me how to bridge research and clinical practice.

To Kaveh, your diligence, insight and enthusiasm helped collect high quality data during testing and helped secure the success of this experiment, while ensuring participants were comfortable. I'd also like to thank our practicum students Cameron Mitchell, Evan Jette, Jade Fraser as well as Emily Koch for helping with testing and fine-tune the experiment. To my friends

and family, thank you for believing in me and giving me the support I needed to realize this dream. We knew that someday our hard work would all pay off; through everyone's individual and collective efforts, now it has – for this, I am grateful.

ABSTRACT

INTRODUCTION: The crural diaphragm electromyogram (EMG_{DIA}), recorded from a multipair esophageal electrode catheter, is often used to assess for changes in central inspiratory neural drive in human subjects under a variety of physiological and/or clinical conditions. Compared to healthy controls, the level of EMG_{DIA} needed to support a given ventilation (V'_E) during exercise is consistently higher in people with chronic obstructive or restrictive pulmonary disease. Studies have also demonstrated that EMG_{DIA}-V'_E relationships are elevated during exercise (i) in the presence compared to absence of a mild restrictive lung deficit caused by external thoracic restriction; (ii) in healthy women compared to men; and (iii) in older compared to younger adults. In all cases, the exaggerated EMG_{DIA}-V'_E response to exercise was accompanied by adoption of a more tachypneic breathing pattern, as well as greater mechanical constraints on tidal volume expansion (V_T) as evidenced by higher dynamic end-inspiratory lung volumes (EILV) or lower inspiratory reserve volumes (IRV). The extent to which these differences in breathing pattern and/or the behaviour of dynamic EILV (or IRV) are responsible for differences in the EMG_{DIA}-V'_E remains unclear.

PURPOSE: To examine the effect of changes in breathing pattern and EILV on neural activation of the crural diaphragm (EMG_{DIA}) and of selected extra-diaphragmatic inspiratory muscles, including the sternocleidomastoid (EMG_{SCM}), scalene (EMG_{SCA}) and external intercostals (EMG_{INT}).

METHODS: Twelve healthy adults aged 25.1±1.6 years (mean±SEM) performed a series of 30-sec breathing trials at a constant V'_E corresponding to 15% of their maximum voluntary V'_E while (i) altering breathing pattern at a constant EILV and (ii) altering EILV at a constant breathing pattern. Using a real-time visual display of each participant's spirogram, EILV was voluntarily targeted at 65% ($EILV_{65\%}$), 75% ($EILV_{75\%}$), 85% ($EILV_{85\%}$) and 95% ($EILV_{95\%}$) of each

participant's inspired vital capacity, while breathing frequency (f_R) was targeted at 15, 35 and 50 breaths/min using a metronome. The V_T needed for a participant to maintain a constant V'_E across trials was achieved *via* changes in end-expiratory lung volume (EELV). A multipair esophageal electrode-balloon catheter was used to record EMG_{DIA} as well as esophageal (Pes) and transdiaphragmatic pressure (Pdi), while skin surface electrodes were used to record EMG_{SCM}, EMG_{SCA} and EMG_{INT}.

RESULTS: Mean values of EMG_{DIA}, EMG_{SCM}, EMG_{SCA} and EMG_{INT} increased as a function of increasing EILV at constant V'_E, independent of changes in breathing pattern and EELV. The magnitudes of these changes were markedly higher in the transition from $EILV_{85\%}$ to $EILV_{95\%}$, especially for EMG_{SCM} and EMG_{SCA}. The relative contributions of EMG_{DIA} and EMG_{INT} to an estimate of global or total central inspiratory neural drive (IND_{TOT}, calculated as the sum of EMG_{DIA}, EMG_{SCM}, EMG_{SCA} and EMG_{INT}) decreased progressively with increasing EILV, while the relative contributions of EMG_{SCM} and EMG_{SCA} to IND_{TOT} increased progressively with increasing EILV. Neuromuscular coupling of the diaphragm and of the respiratory system (quantified as the ratio of peak tidal inspiratory Pdi to EMG_{DIA} and peak tidal inspiratory Pes to IND_{TOT}, respectively) deteriorated progressively with increasing EILV at a constant V'_E, independent to changes in breathing pattern and EELV.

CONCLUSIONS & IMPLICATIONS: In human subjects, as EILV increased towards total lung capacity and V_T was forced to expand on the uppermost (non-compliant) portion of the respiratory systems' sigmoid pressure-volume curve, (i) progressive compensatory (reflex) increases in central inspiratory neural drive to the diaphragm and extra-diaphragmatic inspiratory muscles were required to generate the intrathoracic pressures needed to support V'_E, independent of breathing pattern and EELV; (ii) progressive preferential recruitment of the sternocleidomastoid and scalene muscles helped generate the intrathoracic pressures needed to maintain a constant V'_E and prevent

excessive loading, weakening and neuromuscular uncoupling of the diaphragm; and (iii) progressive neuromuscular uncoupling of the diaphragm and of the respiratory system occurred.

The collective results of this study are unique and revealed the importance of EILV (and unimportance of breathing pattern and EELV) in determining the level of central inspiratory neural drive required to generate inspiratory pressure and support V'_E. These findings have potentially important implications for the assessment and interpretation of respiratory muscle function and activation under a variety of conditions (e.g., rest, sleep, exercise, medical intervention) in health and disease.

RÉSUMÉ SCIENTIFIQUE

INTRODUCTION: L'électromyogramme du diaphragme crural (EMG_{DIA}), enregistré à partir d'un cathéter à électrodes œsophagien à paires multiples, est souvent utilisé pour évaluer les changements de la pulsion inspiratoire du système nerveux central chez les sujets humains dans diverses conditions physiologiques et/ou cliniques. Dans les participants en santé, le niveau d'EMG_{DIA} nécessaire pour soutenir une certaine ventilation (V'_E) pendant l'exercice est régulièrement plus élevé chez les personnes souffrant de maladie pulmonaire obstructive ou restrictive chronique. Des études antérieures ont aussi démontré que le rapport EMG_{DIA}-V'_E est plus élevé pendant l'exercice (i) dans la présence comparée à l'absence d'un léger déficit pulmonaire restrictif causé par une restriction thoracique externe; (ii) chez les femmes en bonne santé comparées aux hommes ; et (iii) chez les adultes plus âgés comparé aux adultes plus jeunes. Dans tous les cas, la réponse exagérée de l'EMG_{DIA}-V'_E à l'exercice est accompagnée par l'adoption d'un profil respiratoire plus tachypnéique, ainsi que des limitations mécaniques pulmonaires plus graves sur l'expansion du volume courant (VC), comme en témoignent les volumes inspiratoires finaux (VFI) dynamiques plus élevés ou les volumes de réserve inspiratoire (VRI) diminués. La mesure dans laquelle ces différences dans le profil respiratoire et/ou le comportement des VFI dynamiques (ou VRI) sont responsables des différences dans l'EMG_{DIA}-V'_E reste incertaine.

OBJECTIF: D'examiner l'effet des changements du profil respiratoire et du VFI sur l'activation neurale du diaphragme crural (EMG_{DIA}) et de certains muscles inspiratoires extradiaphragmatiques, y compris le muscle sterno-cléido-mastoïdien (EMG_{SCM}), les scalènes (EMG_{SCA}) et les muscles intercostaux externes (EMG_{INT}).

MÉTHODES: Douze adultes en bonne santé âgés de 25.1 ± 1.6 ans (moyenne ± SEM) ont effectué une série d'essais respiratoires de 30 secondes, en maintenant une V'_E constante correspondant à 15% de leur ventilation volontaire maximale tout en (i) modifiant le profil

respiratoire à un V'_E constant et (ii) modifiant le VFI à un profil respiratoire constant. En utilisant un affichage visuel en temps réel du spirogramme de chaque participant, le V'_E a été volontairement ciblé à 65 % ($VFI_{65\%}$), 75 % ($VFI_{75\%}$), 85 % ($VFI_{85\%}$) et 95 % ($VFI_{95\%}$) de la capacité vitale inspirée de chaque participant, tandis que la fréquence respiratoire (f_R) a été ciblée à 15, 35 et 50 respirations/min à l'aide d'un métronome. Le VC nécessaire à un participant pour maintenir une V'_E constante d'un essai à l'autre a été obtenue par des changements du volume expiratoire final (VFE). Un cathéter oesophagien à électrodes-ballons à paires multiples a été utilisé pour enregistrer l'EMG_{DIA} ainsi que la pression oesophagienne (Pes) et transdiaphragmatique (Pdi), tandis que des électrodes de surface de la peau ont été utilisées pour enregistrer l'EMG_{SCM}, l'EMG_{SCA} et l'EMG_{INT}.

RÉSULTATS: Les valeurs moyennes de l'EMG_{DIA}, de l'EMG_{SCM}, de l'EMG_{SCA} et de l'EMG_{INT} ont augmenté en fonction de l'augmentation de la VFI à V'_E constant, indépendamment des changements du profil respiratoire et de la VFE. L'ampleur de ces changements a été nettement plus importante lors de la transition de $VFI_{85\%}$ à $VFI_{95\%}$, en particulier pour l'EMG_{SCM} et l'EMG_{SCA}. Les contributions relatives de l'EMG_{DIA} et de l'EMG_{INT} à une estimation de la pulsion inspiratoire du système nerveux central globale ou totale (IND_{TOT}, calculée comme la somme de l'EMG_{DIA}, de l'EMG_{SCM}, de l'EMG_{SCA} et de l'EMG_{INT}) ont diminué progressivement avec l'augmentation du VFI, tandis que les contributions relatives de l'EMG_{SCM} et de l'EMG_{SCA} à l'IND_{TOT} ont augmenté progressivement avec l'augmentation du VFI. Le couplage neuromusculaire du diaphragme et du système respiratoire (quantifié comme étant le ratio du le Pdi au pic inspiratoire par rapport à l'EMG_{DIA} et le Pes au pic inspiratoire par rapport à l'IND_{TOT}, respectivement) se détériore progressivement avec l'augmentation de la VFI à un V'_E constant, indépendamment des changements du profil respiratoire et de la VFE.

CONCLUSIONS ET IMPLICATIONS CLINIQUES: Chez les sujets humains, alors que la VFI augmentait vers la capacité pulmonaire totale et qu'elle se retrouve sur la partie la plus haute (non conforme) de la courbe pression-volume sigmoïde du système respiratoire, (i) des augmentations compensatoires (réflexes) progressives de la commande neurale inspiratoire centrale vers le diaphragme et les muscles inspiratoires extradiaphragmatiques étaient nécessaires pour générer les pressions intrathoraciques nécessaires pour soutenir la V'_E, indépendamment du profil respiratoire et de la VFI; (ii) le recrutement préférentiel progressif des muscles sterno-cléido-mastoïdiens et scalènes a permis de générer les pressions intrathoraciques nécessaires pour maintenir un V'_E constant et prévenir une charge excessive, un affaiblissement et un découplage neuromusculaire du diaphragme ; et (iii) un découplage neuromusculaire progressif du diaphragme et du système respiratoire s'est produit.

Les résultats collectifs de cette étude sont uniques et ont révélé l'importance du VFI (et la non-importance du profil respiratoire et du VEF) dans la détermination du niveau de la pulsion inspiratoire du système nerveux central nécessaire pour générer la pression inspiratoire et soutenir la V'_E. Ces résultats ont des implications potentiellement importantes pour l'évaluation et l'interprétation de la fonction et de l'activation des muscles respiratoires dans diverses conditions (par exemple, repos, sommeil, exercice, intervention médicale) en matière de santé et de maladie.

CHAPTER 1

1.0 Neuro-Respiratory Physiology Background

1.1 Measuring human diaphragm activity as an index of central inspiratory neural drive

In view of the fact that direct measures of phrenic nerve activity are not feasible in human studies, multipair esophageal electrode catheter-derived measures of electromyographic activity of the crural diaphragm (EMG_{DIA}) are often considered the gold standard in obtaining an objective measure of central inspiratory neural drive in human subjects. The physiological basis for use of EMG_{DIA} as an index of central inspiratory neural drive is that the diaphragm receives motor innervation from the phrenic nerve, and there is a strong positive correlation (r=0.82-0.95) between simultaneously measured changes in EMG_{DIA} and phrenic nerve EMG during normal and obstructed breathing [4-6].

As illustrated in Fig. 1.1, combining breath-by-breath measures of EMG_{DIA} along with simultaneous recordings of respired airflow and respiratory muscle pressure development permits detailed examination of the inter-relationships between central inspiratory neural drive, ventilation (V'_E), breathing pattern, operating lung volumes and respiratory muscle pressure development. Indeed, multipair esophageal electrode catheter-derived measures of EMG_{DIA} have been used in: (i) sleep medicine laboratories to assess the role of central inspiratory neural drive in sleep disorder breathing [7-17]; (ii) intensive care units to optimize mechanical ventilation [18-26]; and (iii) clinical exercise and respiratory physiology laboratories

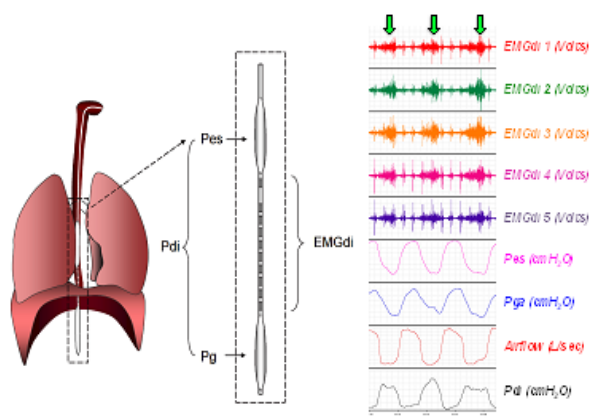

Fig. 1.1 – Combined multipair esophageal electrode catheter, pressure, and flow recordings.

to better understand the neurophysiological mechanisms of breathlessness in health and disease [15, 27-37].

The level of EMG_{DIA} needed to support a given V'_E during exercise is markedly higher in people with obstructive or restrictive pulmonary disorders compared to healthy age- and sex-matched adults [27, 32, 38, 39]. Studies have also shown that EMG_{DIA}-V'_E relationships are elevated throughout exercise (i) in the presence compared to absence of external thoracic restriction in healthy men [40]; (ii) in healthy women compared to men [31, 33]; and (iii) in healthy older compare to younger adults [31]. In all cases, the exaggerated EMG_{DIA}-V'_E response to exercise was accompanied by (i) breathing at a higher end-inspiratory lung volume (EILV) or lower inspiratory reserve volume (IRV) and (ii) adoption of a more tachypneic breathing pattern [27, 29, 31-33, 38-40]. For example, Fig. 1.2 illustrates how EMG_{DIA}-V'_E relationships were higher in the setting of lower IRVs and more tachypneic breathing patterns throughout incremental cycle exercise testing in people with chronic obstructive pulmonary disease (COPD) or interstitial lung disease (ILD) compared to health controls [27]. In keeping with these observations, a study

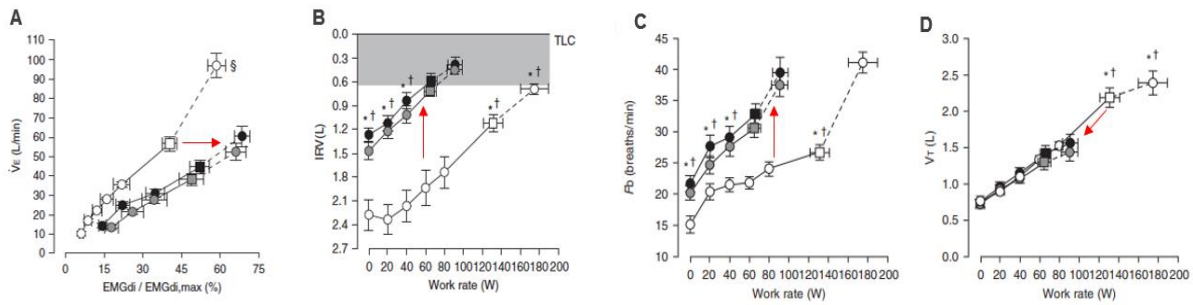

Fig. 1.2 – (A) Relationship between increasing neural drive on ventilation (V'_E) in ILD (grey marker), COPD (black marker) and healthy controls (open marker); (B,C & D) effect of increasing work rate (W) on IRV, F_b and V_T in people with ILD, COPD and healthy controls. $EMG_{di}/EMG_{di,max}$, inspiratory neural drive expressed as a % of maximum activation; V'_E, ventilation; IRV, inspiratory reserve volume; F_b, Breathing frequency. Adapted from Faisal et al. [33].

from our laboratory by Mendonca et al. [40] found that a mild restrictive lung deficit induced by chest-wall strapping (CWS) in healthy men increased the EMG_{DIA}-V'_E response to incremental cycle exercise testing coincident with adoption of a tachypneic breathing pattern and reduced

dynamic IRV (Fig. 1.3). The extent to which these differences in breathing pattern and/or the behaviour of dynamic EILV (or IRV) are responsible for differences in the EMG_{DIA}-V'_E remains unclear and represents the focus of this thesis. What follows is a brief description of the physiological basis for how adopting a tachypneic breathing pattern or breathing at an abnormally high EILV (or abnormally low IRV) might necessitate an exaggerated level of central inspiratory neural drive to support a given V'_E.

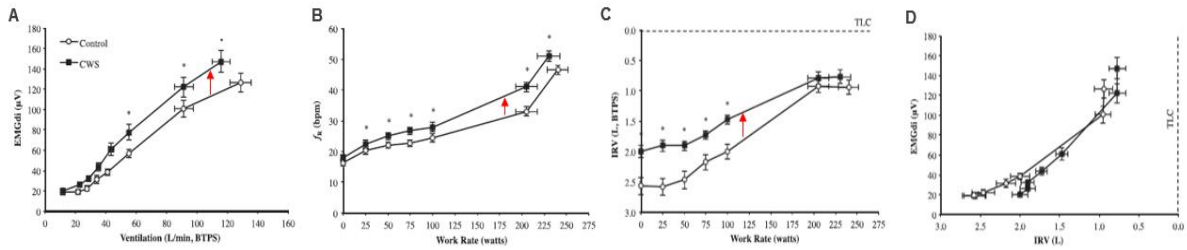

Fig. 1.3 – Effect of chest wall strapping (CWS) vs. unobstructed breathing (control) on (A); EMG_{DIA}-V'_E; (B) f_R-work rate, (C); IRV-work rate and (D); EMG_{DIA}-IRV. EMG_{di} (µV), units expressed in micro volts; f_R, breathing frequency; IRV, inspiratory reserve volume. Adapted from Mendonca et al. [39].

1.12 Diaphragm muscle physiology

Basic principles of skeletal muscle physiology predict that, at constant level of neural activation, the maximal force output of a muscle will decrease as its (i) sarcomeres shorten beyond an optimal position and (ii) velocity of shortening or contraction increases [41].

As with all skeletal muscles, the maximal pressure generating capacity of the diaphragm falls as its length decreases. For example, during inspiration at high lung volumes, the diaphragm contracts (shortens) and descends down into the abdomen. As illustrated in Fig. 1.4a, this would be expected to decrease pressure generating capacity of the diaphragm by decreasing the length of the diaphragm's sarcomeres below their optimal length [42]. Indeed, Fig. 1.4b highlights a roughly proportional decline in diaphragm pressure generating capacity (as estimated by changes in transdiaphragmatic pressure (Pdi)) and diaphragm length whilst breathing at lung volumes from residual volume (RV) to total lung capacity (TLC) [43-45].

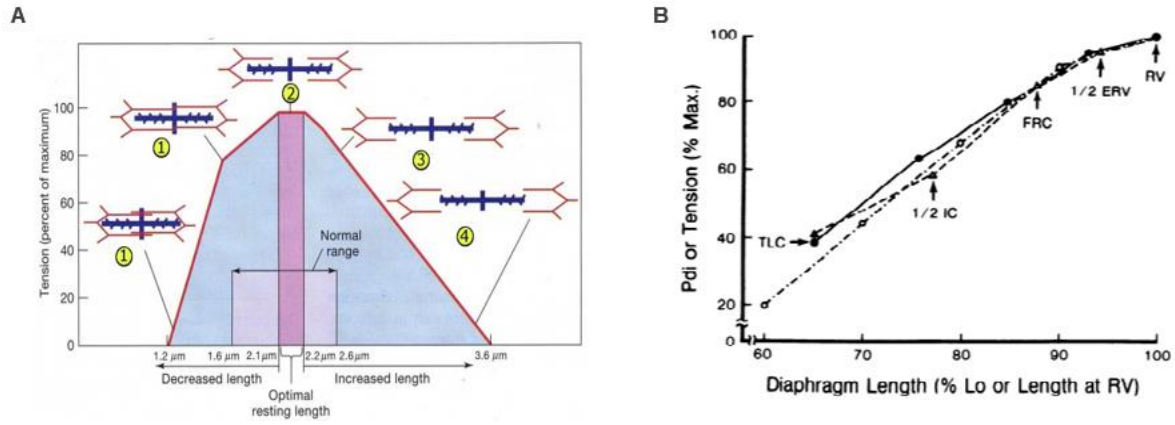

Fig. 1.4 – (A) AV Hill's representation of the sarcomere length-tension relationship [52]; (B) Effect of diaphragm length on inspiratory force generation capacity (Pdi). Adapted from Smith and Bellemare [44].

Studies have also confirmed basic principles of myofibrillar contractile performance in terms of the velocity of shortening and similarly noted how the capacity of the inspiratory muscles to generate pressure falls with increasing inspiratory flow [46, 47]. While an increased inspired flow rate is clearly indicative of an increased velocity of inspiratory muscle contraction, increases in EILV provide information about the length/curvature of the diaphragm (as EILV increases, diaphragm length decreases) as well as the extent of inspiratory elastic loading associated with breathing on the upper alinear portion of the respiratory systems' sigmoid pressure-volume curve (as EILV increases, inspiratory elastic loading increases). Thus, breathing at a high EILV is associated with both an increased demand and decreased capacity of the diaphragm to generate negative inspiratory pressure and support V'_E.

In its simplest form, diaphragm myofibrillar contractile performance fundamentally reflects the cross-cycling between (i) the force-generating state, where actin and myosin are tightly bound and (ii) the non-force generating state, where cross bridges are detached from actin; both could be independently influenced by alterations in breathing pattern or EILV [44-46]. However, 'global inspiratory demands' are matched not only by the diaphragm's pressure generating capacity but also the pressure generating capacity of extra-diaphragmatic inspiratory muscles (e.g.,

sternocleidomastoid (SCM), scalene (SCA) and external intercostal muscles (INT)), whose function is also influenced by changes in inspiratory flow and lung volume (*see Section 1.4 below*).

1.2 Lung volume physiology - pressure-volume relationships

1.21 Rationale for why lung volume (EILV) might influence EMG_{DIA}-V_E relationships

An important study by Leblanc et al. [46] demonstrated how pressure generating capacity of the inspiratory muscles was relatively well preserved when breathing at lung volumes between 30 and 55% of TLC. However, as illustrated in Fig. 1.5, the effect of increasing lung volume beyond 55% of TLC resulted in a ~ 1.7% decrease in inspiratory muscle pressure generating capacity for every 1% increase in lung volume. It stands to reason, that breathing at lung volumes

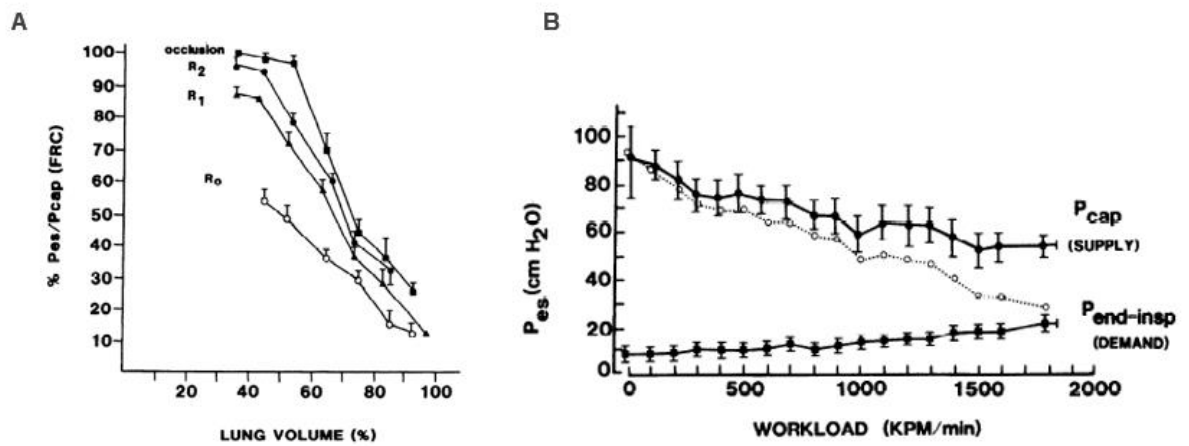

Fig. 1.5 – (A) Effect of increasing lung volume on inspiratory muscle pressure generating capacity at resistance ranging none (open) to occlusion from (0 to 6 L/sec); (B).Increasing workload and lung volume result in a decrease in P_{cap} and supply-demand mismatch. Pes, esophageal pressure; Pcap, maximum inspiratory esophageal pressure; $P_{end\text{-}insp}$, end-inspiratory esophageal pressure. Adapted from Leblanc et al. [42].

close to TLC decreases inspiratory (diaphragm) muscle pressure generating capacity *via* sarcomere shortening. At the same time, breathing at lung volumes close to TLC increases the demand of the inspiratory muscles to generate pressure by forcing V_T to expand on the uppermost (non-compliant) portion of the respiratory systems' sigmoid pressure-volume curve where there is increased inspiratory elastic loading due to recoil of both the lung and chest wall. It is reasonable to assume that, under these circumstances of both increased demand and decreased capacity of the inspiratory muscles to develop pressure whilst breathing at lung volumes close to TLC,

compensatory increases in central inspiratory neural drive to the diaphragm and extra-diaphragmatic inspiratory muscles (i.e., increased motor unit recruitment and firing rate) are required to sustain V'_E.

1.3 Breathing pattern physiology - force-velocity relationships

1.31 Rationale for why tachypnea might influence EMG_{DIA}-V'_E relationships

At any given level of V_T expansion, increasing inspiratory flow rate and the velocity of inspiratory muscle contraction (or shortening) will result in a greater proportion of actin-myosin cross-bridges existing in the detached phase (non-force generating). In other words, adoption of a tachypneic breathing pattern has the potential to decrease inspiratory muscle pressure generating capacity by decreasing productive myosin attachment time and contact duty ratio [48]. Indeed, Fig. 1.6 shows how force generating capacity of the inspiratory muscles decreases as a function of increasing inspired flow rate at lung volumes between 40 and 100% of TLC [46]. While many of the maximal inspiratory esophageal pressures, flow and volume derivations were performed in static conditions using mouth occlusion techniques, exercise testing similarly showed how increasing f_R from ~14 breaths/min at rest to ~40 breaths/min at peak exercise resulted in a lower inspiratory muscle pressure generating capacity [46, 49, 50]. It follows that a higher velocity of inspiratory muscle contraction could require a greater level of central inspiratory neural drive to compensate for the combination of both greater in demand and lower capacity of the inspiratory muscles to generate negative inspiratory pressure

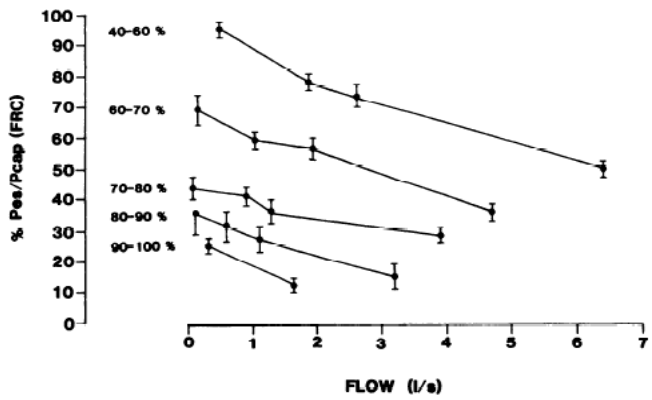

Fig. 1.6 – Effect of varying inspiratory flow on inspiratory muscle pressure generating capacity at lung volumes from 40 to 100% total lung capacity. Pes, esophageal pressure; Pcap, maximum inspiratory esophageal pressure; FRC, functional residual capacity. Adapted from Leblanc et al. [42].

and sustain V'_E. In fact, changes in f_R were recently identified as an possible "*independent' deteriorator"* associated with higher central inspiratory neural drive [51, 52].

1.32 Conflicting evidence for a role of tachypnea in determining EMG_{DIA}-V'_E relationships

While the above-mentioned studies provide evidence linking increased velocity of inspiratory muscle contraction (inspiratory flow) with increased EMG_{DIA} activity, it is worth mentioning that not all studies support such a link [3]. Specifically, Beck et al. [3] reported no change in the level of EMG_{DIA} needed to achieve any given Pdi when healthy participants breathed from functional residual capacity (FRC) to TLC at inspiratory flow rates between 0.1 to 1.4 L/sec (Fig. 1.7). Furthermore, a study by Hussain et al. [1] investigating the neuro-mechanical consequences of rapid (and imperceptible) alterations in pulmonary resistance did not support a link between breathing pattern and EMG_{DIA}. Specifically, as illustrated in Fig. 1.8, rapidly switching the inspired gas from helium (lower density gas with lower pulmonary resistance) to room air (higher density gas with higher pulmonary resistance) was associated with an immediate increase in EMG_{DIA} despite no corresponding change in V_T, f_R, V'_E and Pdi.

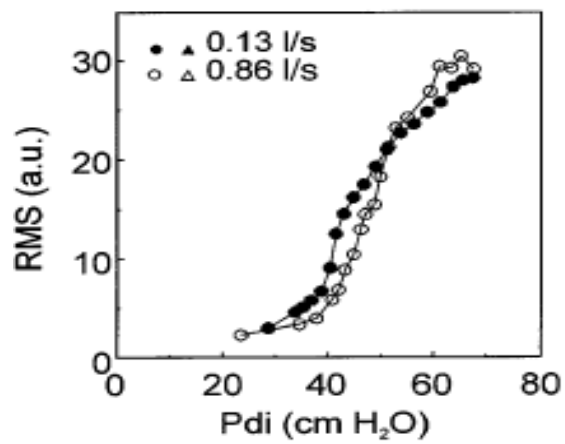

Fig. 1.7 –Effect of increasing transdiaphragmatic force (Pdi) on EMG_{DIA} (RMS in arbitrary units) at slow (dark triangles) and faster (open triangle) velocity of shortening. Adapted from Beck et al. [3].

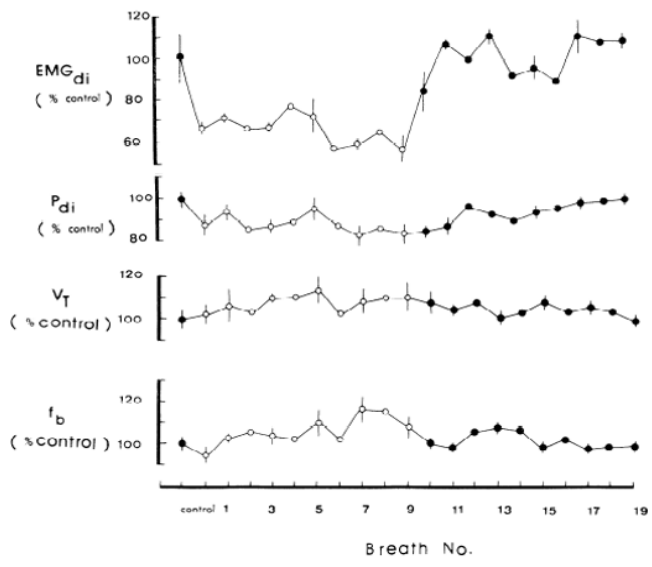

Fig. 1.8 – Physiological consequences of switching from helium (open dots) to room air (dark) on EMGdi, V_T, Pdi and f_R. Adapted from Hussain et al. [1].

1.4 Impact of lung volume and velocity of inspiratory muscle contraction on neural activation of the extra-diaphragmatic inspiratory muscles

Experimental evidence suggests that neural activation of the extra-diaphragmatic inspiratory muscles, particularly the sternocleidomastoid (EMG_{SCM}) and scalene muscles (EMG_{SCA}), is also influenced by changes in the velocity of inspiratory muscle contraction and lung volume. For example, Washino et al. [2] recently reported that EMG_{SCM} and EMG_{SCA} increased as a function of increasing inspiratory flow rate at any given lung volume between 20 and 60% of forced vital capacity, particularly at inspiratory flow rates of ≥40% of peak inspiratory flow rate (Fig. 1.9). A classical study by Raper et al. [53] showed that both EMG_{SCA} and

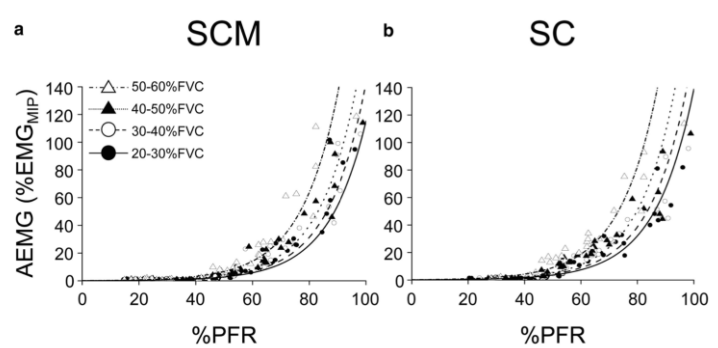

Fig. 1.9 – Relation between increasing inspiratory flow rate normalized to peak inspiratory flow rate (%PFR) on neural activation of the sternocleidomastoid (SCM, left) and scalene (SC, right) muscles at lung volumes between 20% and 60% of forced vital capacity (FVC). Adapted from Washino et al. [2].

EMG_{SCM} activity increased progressively (albeit in different proportions and with different time courses of change) with increasing lung volume until 100% vital capacity was approached, at which point EMG_{SCA} and EMG_{SCM} increased abruptly. In keeping with these observations, Ramsook et al. [54] observed a precipitous rise in both EMG_{SCA} and EMG_{SCM} staring at an EILV of ~80% of TLC during maximal incremental cycle exercise testing in healthy adults (Fig. 1.10).

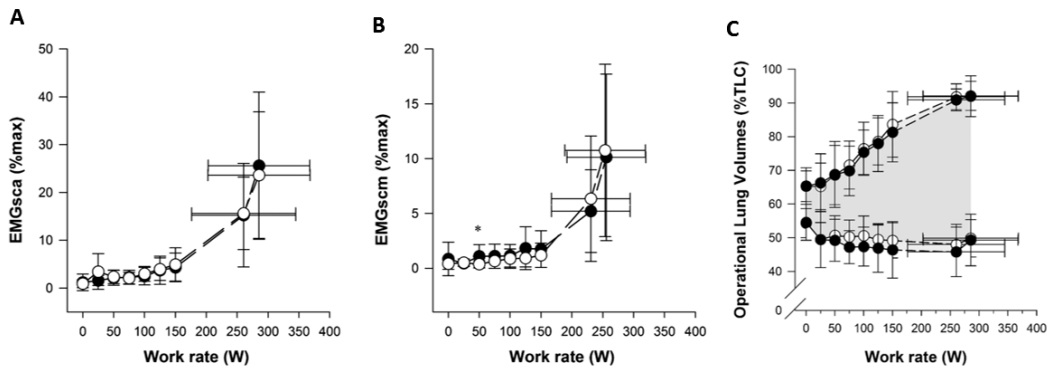

Fig. 1.10 – Effect of increasing work rate during incremental cycle exercise testing on neural activation of the sternocleidomastoid (EMGscm) and scalene (EMGsca) muscles as well as the behaviour of dynamic operating lung volumes in healthy adults. Adapted from Ramsook et al. (2017).

While the influence of breathing pattern (tachypnea) on EMG_{DIA}-V'_E relationship remains unclear, there is consistent evidence that changes in EILV play an important role in the exaggerated EMG_{DIA}-V'_E relationship observed during exercise, for example, in people with COPD or ILD compared to healthy control subjects [27]. Despite the physiological and experimental evidence supporting a role of tachypnea and an elevated EILV on EMG_{DIA}-V'_E relationships, few studies have been able to isolate the independent and/or combined effect of changes in breathing pattern and EILV on the level of central inspiratory neural drive needed to generate negative inspiratory pressure and support V'_E. This is exemplified by the following quote from Leblanc et al. [46]: "*During dynamic muscle action under physiological conditions the effects of length, velocity, frequency, tension, timing, and their interactions on the fatiguing process are difficult to establish independently because of the problem in isolating the effect of changes in any one variable alone.*" As described in Chapter 2, the experimental design of this MSc thesis research project was unique and sought to isolate the effect of changes in breathing pattern and EILV on detailed assessments

of neural activation of the diaphragm and of the extra-diaphragmatic inspiratory muscles at constant V'_E.

1.5 Research aims

As discussed above, abnormalities in the level of central inspiratory neural drive (quantified as EMG activity of the diaphragm and/or extra-diaphragmatic inspiratory muscles) needed to support a given V'_E may be mechanistically linked to adoption of a tachypneic breathing pattern or breathing at an EILV close to TLC. However, the individual and combined effect of alternations in breathing pattern and EILV on inspiratory muscle EMG-V'_E relationships remains unclear. Thus, the primary aim of this study was to the examine the individual and combined effect of alterations in breathing pattern and EILV on the level of EMG_{DIA} needed to support a constant V'_E. The secondary aim was to examine the impact of alterations in breathing pattern and/or EILV at a constant V'_E on the recruitment (activation) pattern of the extra-diaphragmatic inspiratory muscles, specifically the sternocleidomastoid, scalene and external intercostal muscles.

CHAPTER 2

2.1 ABSTRACT

PURPOSE: To purpose of this study was to examine the effect of changes in breathing pattern and end-inspiratory lung volume (EILV) on neural activation of the crural diaphragm (EMG_{DIA}) and of the sternocleidomastoid (EMG_{SCM}), scalene (EMG_{SCA}) and external intercostal muscles (EMG_{INT}). **METHODS:** Twelve healthy adults aged 25.1±1.6 years (mean±SEM) performed a series of 30-sec breathing trials at a constant ventilation (V'_E) corresponding to 15% of their maximum voluntary ventilation while (i) altering breathing pattern at a constant EILV and (ii) altering EILV at a constant breathing pattern. Using a real-time visual display of each participant's spirogram, EILV was voluntarily targeted at 65% ($EILV_{65\%}$), 75% ($EILV_{75\%}$), 85% ($EILV_{85\%}$) and 95% ($EILV_{95\%}$) of each participant's inspired vital capacity, while breathing frequency (f_R) was targeted at 15, 35 and 50 breaths/min using a metronome. The tidal volume needed for a participant to maintain a constant V'_E across trials was achieved *via* changes in end-expiratory lung volume (EELV). A multipair esophageal electrode catheter was used to record EMG_{DIA}, while skin surface electrodes were used to record EMG_{SCM}, EMG_{SCA} and EMG_{INT}. **RESULTS:** On average, EMG_{DIA}, EMG_{SCM}, EMG_{SCA} and EMG_{INT} increased as a function of increasing EILV at constant V'_E, independent of changes in breathing pattern and EELV. The magnitudes of these increases were particularly notable in the transition from $EILV_{85\%}$ to $EILV_{95\%}$, especially for EMG_{SCM} and EMG_{SCA}. **CONCLUSION:** In human subjects, as EILV increases towards total lung capacity, progressive compensatory (reflex) increases in central inspiratory neural drive to the diaphragm and extra-diaphragmatic inspiratory muscles are required to generate the intrathoracic pressures needed to support V'_E, independent of breathing pattern and EELV.

2.2 INTRODUCTION

The crural diaphragm electromyogram (EMG_{DIA}), recorded from a multipair esophageal electrode catheter, is commonly used to assess for changes in central inspiratory neural drive in human subjects under a variety of physiological and/or clinical conditions. For example, EMG_{DIA} has been used in clinical exercise physiology studies to better understand the neurophysiological mechanisms of exertional breathlessness in people with chronic obstructive or restrictive pulmonary disease [15, 27, 32, 38, 55]. The physiological basis for use of EMG_{DIA} as an index of central inspiratory neural drive is that the diaphragm receives motor innervation from the phrenic nerve, and there is a strong positive correlation (r=0.82-0.95) between simultaneously measured changes in EMG_{DIA} and phrenic nerve EMG during normal and obstructed breathing [4-6].

Compared to healthy controls, the level of EMG_{DIA} needed to support a given ventilation (V'_E) during exercise is consistently higher in people with chronic obstructive or restrictive pulmonary disease [27, 32, 38, 56]. Studies have also demonstrated that EMG_{DIA}-V'_E relationships are elevated during exercise in (i) the presence compared to absence of a mild restrictive lung deficit caused by external thoracic restriction [40]; (ii) healthy women compared to men [31, 33]; and (iii) older compared to younger adults [31]. In all cases, the exaggerated EMG_{DIA}-V'_E response to exercise was accompanied by adoption of a more tachypneic breathing pattern, as well as greater mechanical constraints on tidal volume (V_T) expansion as evidenced by higher dynamic end-inspiratory lung volumes (EILV) or lower inspiratory reserve volumes (IRV). The extent to which these differences in breathing pattern and/or the behaviour of dynamic EILV (or IRV) are responsible for differences in the EMG_{DIA}-V'_E relationship is unclear and represents the focus of our study.

Basic principles of muscle physiology predict that maximum force of contraction of a muscle decreases as its velocity of contraction increases and/or its length decreases (sarcomeres shorten). In other words, a short muscle contracting at a high velocity is a “functionally” weak

muscle. Applying these principles to the respiratory system, Leblanc et al. [46] showed that the capacity of the inspiratory muscles to generate pressure falls with increasing inspiratory flow (increasing velocity of contraction) and increasing EILV (decreasing inspiratory muscle length).

Physiologically, EILV provides valuable information about the operating length of the inspiratory muscles and the elastic loads imposed on them. Specifically, as EILV increases, it encroaches on total lung capacity (TLC) and positions itself on the upper alinear (non-compliant) extreme of the respiratory systems' sigmoid pressure-volume curve, where there is both an increase in elastic loading (secondary to decreased lung and chest wall compliance) and a decrease in functional strength of the inspiratory muscles (secondary to decreased operating length), particularly the diaphragm. In light of the above, it is reasonable to hypothesize that compensatory (reflex) increases in central inspiratory neural drive are required to generate the intrathoracic pressures needed to support a given V'_E whilst breathing at a high EILV and/or with a tachypneic breathing pattern.

The primary aim of this study was to the examine the individual and combined effects of alterations in EILV and breathing pattern on the level of EMG_{DIA} needed to support a constant V'_E. Our secondary aim was to examine the impact of alterations in EILV and/or breathing pattern at a constant V'_E on the recruitment (activation) pattern of the extra-diaphragmatic inspiratory muscles, specifically the sternocleidomastoid (EMG_{SCM}), scalene (EMG_{SCA}) and 7th external intercostals (EMG_{INT}).

2.3 METHODS

2.3.1. Study design. This study consisted of a single 3 to 4-hour visit to the *Clinical Exercise & Respiratory Physiology Laboratory* of McGill University. During this visit, eligible participants performed routine pulmonary function tests followed by 12 breathing trials, with each trial performed twice. Participants were asked to avoid alcohol, caffeine and strenuous exercise on the test day; and to refrain from eating a heavy meal within 4 hours before testing. The study protocol and consent form were approved by the Institutional Review Board of the Faculty of Medicine at McGill University (A05-M48-14B) in accordance with the Declaration of Helsinki.

2.3.2. Participants. Participants included apparently healthy, non-smoking, non-obese (body mass index (BMI) <30 kg/m^2) men and women aged 18-40 years with normal spirometry (forced expiratory volume in 1-sec (FEV_1) to forced vital capacity ratio (FVC) >0.70 and FEV_1 ≥80% predicted [57]) and who were not taking any doctor prescribed medications, other than oral contraceptives. Participants were recruited from Montréal and surrounding areas by word of mouth and posted announcements.

2.3.3. Pulmonary function tests. Spirometry and 15-sec maximum voluntary ventilation (MVV) maneuvers were performed with participants seated upright using automated testing equipment (SensorMedics Vs229d, Yorba Linda, CA) in accordance with recommended techniques [23]. Spirometric parameters were referenced to their normal predicted values [57].

2.3.4. Breathing trials. Breathing trials were performed with participants (i) seated on a chair in an upright position with back supported and arms in a relaxed and steady position and (ii) breathing through a rubber mouthpiece connected in series to a microbial filter (part no: V-892384, MicroGard IIC; Vyaire Medical, Inc., Mettawa, IL, USA) and low-resistance flow sensor with

nasal passages occluded by a nose-clip. Each trial was 30-sec in duration and interspersed by at least 1-min of rest. The order of the trials was randomized for each participant using an online randomization software (www.randomizer.com).

Breathing trials were performed at (i) a constant V'_E corresponding to 15% of each participant's MVV, rounded up to the nearest 5 L/min increment; (ii) standardized breathing frequencies of 15 ($f_{R,15}$), 35 ($f_{R,35}$) and 50 breaths/min ($f_{R,50}$), with each participant's V_T adjusted to each of the breathing frequencies so as to maintain V'_E constant at 15% of MVV; and (iii) standardized EILVs corresponding to 65% ($EILV_{65\%}$), 75% ($EILV_{75\%}$), 85% ($EILV_{85\%}$) and 95% ($EILV_{95\%}$) of each participant's inspired vital capacity (IVC), which was determined prior to the start breathing trials. The V_T needed for a participant to generate a constant V'_E at a given f_R and EILV was achieved *via* changes in their end-expiratory lung volume (EELV). Table 2.1 presents the targeted levels of V'_E, f_R, V_T, EILV and EELV for each of the 12 breathing trials for a hypothetical participant with an IVC of 6 L and MVV of 165 L/min.

Table 2.1. Example of the targeted levels of ventilation (V'_E), breathing frequency (fR), tidal volume (V_T), end-inspiratory lung volume (EILV) and end-expiratory lung volume (EELV) for each of the 12 breathing trials for a hypothetical participant with an inspired vital capacity (IVC) of 6 L and a maximum voluntary ventilation of 165 L/min.

	V'_E = 25 L/min f_R = 15 bpm V_T = 1.67 L	V'_E = 25 L/min f_R = 35 bpm V_T = 0.71 L	V'_E = 25 L/min f_R = 50 bpm V_T = 0.50 L
$EILV_{65\%}$ of IVC and EELV (L)	3.90 and 2.23	3.90 and 3.19	3.90 and 3.40
$EILV_{75\%}$ of IVC and EELV (L)	4.50 and 2.83	4.50 and 3.79	4.50 and 4.00
$EILV_{85\%}$ of IVC and EELV (L)	5.10 and 3.43	5.10 and 4.39	5.10 and 4.60
$EILV_{95\%}$ of IVC and EELV (L)	5.70 and 4.03	5.70 and 4.99	5.70 and 5.20

Trials were performed with participants seated in front of a 27" television monitor displaying their spirogram so that breath-by-breath changes of their EILV and EELV could be visualized. Participants were instructed to inspire to a given EILV and expire to a given EELV by targeting horizontal (visual) guidelines set on the monitor, while simultaneously pacing their breathing at 15, 35 or 50 breaths/min according to audible tones generated by a metronome for

inspiration and expiration in a 1:1 ratio. Maximum voluntary inspiratory capacity maneuvers (IC) were performed immediately before and immediately after each trial. We verified that maximal inhalation volume (or TLC) was attained during both IC maneuvers by confirming that peak inspiratory (negative) esophageal pressure values were closely matched.

Airflow and respired PCO_2 were measured using a SensorMedics V*s229*d metabolic cart (Yorba Linda, CA, USA). The flow sensor and gas analyzer were calibrated prior to the start of breathing trials using a 3 L syringe and known concentrations of compressed gas, respectively. The continuous airflow (integrated over time to provide volume) and respired PCO_2 signals from the *V*s229d system were simultaneously input into a PowerLab 16/30 analog-to-digital converter (model ML880) running LabChart Pro Version 8.1.5 software (ADInstruments, Castle Hill, Australia) and sampled at 200 Hz. Heart rate (HR) and blood O_2 saturation (SpO_2) were assessed by finger pulse oximetry (Capnocheck Plus Capnograph®, Smiths Medical ASD, Inc. Norwell, MA, USA).

To help minimize drift in the integrated flow (volume) trace used for prospective targeting of EILV and EELV, corrections were developed to account for electrical changes over time, non-linearity in the flow sensor, and differences in gas temperature and humidity. The combination of (i) these corrective measures, (ii) the short 30-sec duration of each trial, and (iii) close matching of inspired and expired volumes during each trial resulted in relatively small amounts of drift (i.e., ≤5% difference in maximal inhalation volume recording during paired-IC maneuvers performed before and after each trial).

Drift in the integrated flow (volume) tracing was corrected for analysis of ventilatory parameters by performing an interpolated volume correction between the two maximal inhalation volumes obtained during paired-IC maneuvers performed before and after each trial [58]. The drift-corrected volume tracing was then used to identify EILV and EELV. Tidal volume was then calculated as the difference between EILV and EELV, while V'_E was calculated as the product of

V_T and f_R. Inspiratory reserve volume (IRV) was calculated as the difference between IVC and EILV. Total respiratory cycle duration (T_{TOT}) was taken as the sum of inspiratory time (T_I) and expiratory time (T_E), which were identified as the duration of time between points of zero flow. Inspiratory duty cycle was calculated as the ratio of T_I to T_{TOT} (T_I/T_{TOT}), while mean tidal inspiratory flow was calculated as the ratio of V_T to T_I (V_T/T_I) and used as an index of the velocity of inspiratory muscle contraction. End-tidal PCO_2 ($P_{ET}CO_2$) was identified as the peak PCO_2 recorded during tidal expiration.

2.3.5. Inspiratory muscle EMG – measurement and analysis: Breath-by-breath measures of EMG_{DIA} were recorded from a multipair esophageal electrode-balloon catheter (Guangzhou Yinghui Medical Equipment, Guangzhou, China). As described in detail elsewhere [59], the catheter consists of ten 1-cm silver coils that form five consecutive EMG_{DIA} recording pairs as well as an esophageal and gastric balloon for measurement of respiratory pressures. After numbing of the nasal and pharyngeal passages with a 2% endotracheal lidocaine spray (Lidodan™ Endotracheal Non-Aerosol Spray; Odan Laboratories Ltd., Montréal, QC, Canada), the electrode-balloon catheter was passed through the nose and positioned according to established methods [29, 60]. Briefly, the position of the electrode catheter was known to be optimal when the amplitude of EMG_{DIA} recorded during tidal inspiration was greatest in electrode pairs 1 and 5, and lowest in electrode pair 3. Once optimally positioned, the electrode catheter was fixed externally the nose.

Bipolar skin surface electrodes (Noraxon Dual Hex Electrodes, model 272(s), Scottsdale, AZ, USA) were used to record breath-by-breath changes in EMG_{SCM}, EMG_{SCA} and EMG_{INT} according to recommendations for proper use of transcutaneous EMG for non-invasive assessment of muscles [61], including extra-diaphragmatic inspiratory muscles [62]. The positions of the EMG_{SCM} and EMG_{SCA} electrodes were based on the work of Ramsook et al. [54], while the position of the EMG_{INT} electrodes were based on the work of Guenette et al. [63]. Non-obese participants with a BMI <30

kg/m^2 were purposefully studied to minimize the potential for attenuation of EMG signal strength/quality from subcutaneous adipose tissue overlying each of the extra-diaphragmatic inspiratory muscles. To minimize the potential for crosstalk contamination of EMG_{SCA} from EMG_{SCM}, we confirmed a marked increase in EMG_{SCM} without a corresponding change in EMG_{SCA} during maximal voluntary contralateral rotations of the head against resistance prior to the start of breathing trials in each participant.

All raw EMG data were sampled continuously at 2,000 Hz using a PowerLab 16/30 analog-to-digital converter (model ML880) running LabChart Pro Version 8.1.5 software (ADInstruments, Castle Hill, Australia); and amplified and band-pass filtered between 20 and 1,000 Hz (model RA-8; Guangzhou Yinghui Medical Equipment Ltd., Guangzhou, China).

All raw EMG data were converted to root mean square ($EMG_{DIA,rms}$, $EMG_{SCM,rms}$, $EMG_{SCA,rms}$ and $EMG_{INT,rms}$) using a time constant of 100-msec and a moving window (LabChart Pro Version 8.1.5, ADInstruments). The maximum root mean square value during 100-msec subdivisions of each inspired breath was determined by manually selecting $EMG_{DIA,rms}$, $EMG_{SCM,rms}$, $EMG_{SCA,rms}$ and $EMG_{INT,rms}$ signals falling between QRS complexes so as to avoid contamination from cardiac artifact. The electrode pair with the largest $EMG_{DIA,rms}$ amplitude for each inspired breath was used for analysis. The sum of $EMG_{DIA,rms}$, $EMG_{SCM,rms}$, $EMG_{SCA,rms}$ and $EMG_{INT,rms}$ was used as an unvalidated estimate of global or total central inspiratory neural drive ($IND_{TOT,rms}$).

2.3.6. Respiratory pressures – measurement and analysis: Esophageal and gastric balloons were filled with 0.5 mL and 1.2 mL of air, respectively. Esophageal (Pes), gastric (Pga) and transdiaphragmatic pressures (Pdi = Pga – Pes) were sampled continuously at 200 Hz using a PowerLab 16/30 analog-to-digital converter (model ML880) running LabChart Pro Version 8.1.5 software (ADInstruments); calibrated differential pressure transducers (model DP15-34; Validyne Engineering, Northridge, CA, USA); and a signal conditioner (model CD280-4; Validyne Engineering).

Tidal Pes swings (Pes,tidal) were calculated as the difference between peak tidal inspiratory (Pes,inspir) and expiratory Pes. Tidal Pdi swings (Pdi,tidal) were similarly calculated as the difference between peak tidal inspiratory (Pdi,inspir) and expiratory Pdi. The ratio of Pdi,inspir to $EMG_{DIA,rms}$ was used as an index of neuromuscular coupling of the diaphragm, while the ratio of Pes,inspir to $IND_{TOT,rms}$ was used as an index of neuromuscular coupling of the respiratory system.

2.3.7. Statistical analysis. Physiological parameters measured breath-by-breath were averaged over the last 5 breaths of each 30-sec breathing trial. These parameters were linked with HR and SpO_2 values recorded at the end of each trial. All physiological parameters were averaged across the first and second iteration of each breathing trial and used for statistical analysis.

A two-way repeated measures analysis of variance with Tukey's HSD post-hoc test was used to examine the effect of breathing pattern and $EILV_{\%IVC}$ on measured parameters (SigmaStat Version 3.5, Systat Software Inc., San Jose, CA, USA). Statistical significance was set at $p<0.05$. Data are reported as mean ± standard error of the mean (SEM).

2.4 RESULTS

2.4.1. Participant characteristics. Sixteen participants consented to participate in this study; however, four were excluded because they: were unable to match their breathing to the targeted f_R and/or $EILV_{\%IVC}$ (n=2); did not tolerate the esophageal catheter (n=1); and had a FEV_1/FVC <0.70 (n=1). The final sample included 7 men and 5 women described in Table 2.2.

Table 2.2. Participant characteristics

Age (years) [range]	25.1 ± 1.6 [21-40]
Body mass index (kg/m^2) [range]	24.0 ± 0.7 [20-29]
FEV_1 (L) [% predicted]	4.61 ± 0.27 [107 ± 3]
FVC (L) [% predicted]	5.58 ± 0.34 [109 ± 3]
FEV_1/FVC (%)	83 ± 1
$FEF_{25-75\%}$ (L/sec) [% predicted]	4.81 ± 0.35 [105 ± 6]
MVV (L/min)	179 ± 15

Values are means ± SEM. ***Abbreviations***: FEV_1, forced expiratory volume in 1-sec; FVC, forced vital capacity; $FEF_{25-75\%}$, forced expiratory flow between 25% and 75% of FVC maneuver; MVV, maximum voluntary ventilation.

2.4.2. Breathing trials – physiological responses. Participants' matched their EILV to the targeted values of 65%, 75%, 85% and 95% of IVC at each f_R (Fig. 2.1A, Table 2.3). Likewise, f_R was well matched to the targeted values of 15, 35 and 50 breaths/min at each $EILV_{\%IVC}$ (Fig. 2.1B, Table 2.3). Participants maintained a relatively constant V'_E of ~15%MVV (or ~30 L/min) across all breathing trials, except at $f_{R,50}$ where V'_E was modestly but significantly greater (by ~2%MVV or ~3 L/min) at $EILV_{95\%}$ compared to $EILV_{65\%}$, $EILV_{75\%}$ and $EILV_{85\%}$ (Fig. 2.2A, Table 2.3). As expected, V_T was significantly different across f_R conditions ($f_{R,15} > f_{R,35} > f_{R,50}$), but maintained relatively constant across $EILV_{\%IVC}$ trials, with the exception of V_T being significantly greater (by 0.05 L) at $EILV_{95\%}$ compared to $EILV_{65\%}$ when breathing at $f_{R,50}$ (Fig. 2.2B, Table 2.3). Within any given $EILV_{\%IVC}$ condition, differences in V_T across f_R conditions were due to differences in EELV ($f_{R,15} < f_{R,35} < f_{R,50}$) (Table 2.3). Heart rate was similar across all breathing trials, except at $f_{R,35}$ and $f_{R,50}$ where HR was significantly higher at $EILV_{95\%}$ compared to $EILV_{65\%}$, $EILV_{75\%}$ and $EILV_{85\%}$ (Table 2.3). There was no difference in $P_{ET}CO_2$ (Fig. 2.2C), SpO_2 and T_I/T_{TOT} across all trials (Table 2.3). On average, V_T/T_I was not significantly different across f_R conditions within any given $EILV_{\%IVC}$ condition, but was significantly higher at $EILV_{95\%}$ compared to $EILV_{65\%}$, $EILV_{75\%}$ and $EILV_{85\%}$ within each of the f_R conditions (Fig. 2.2D, Table 2.3).

2.4.3. Breathing trials – Inspiratory muscle EMG and respiratory pressure responses. Mean values of $EMG_{DIA,rms}$ (Fig. 2.3A), $EMG_{SCM,rms}$ (Fig. 2.3B), $EMG_{SCA,rms}$ (Fig. 2.3C), $EMG_{INT,rms}$ (Fig. 2.3D) and $IND_{TOT,rms}$ (Fig. 2.4A) increased progressively with increasing $EILV_{\%IVC}$ (particularly in the transition from $EILV_{85\%}$ to $EILV_{95\%}$), independent of f_R or breathing pattern (Table 2.3).

Because f_R had no effect on the relationship between $EILV_{\%IVC}$ and either one of the inspiratory muscle group EMG responses, the effect of increasing $EILV_{\%IVC}$ on the absolute (Fig.

2.4B) and relative contributions (Fig. 2.4C) of $EMG_{DIA,rms}$, $EMG_{SCM,rms}$, $EMG_{SCA,rms}$ and $EMG_{INT,rms}$ to $IND_{TOT,rms}$ were quantified for each participant by collapsing (averaging) data across the f_R conditions within each of the $EILV_{\%IVC}$ conditions. A one-way repeated measures analysis of variance with Tukey's HSD post-hoc test was then used to examine the impact of increasing $EILV_{\%IVC}$ on the relative contribution of each inspiratory muscle group's EMG activity to $IND_{TOT,rms}$. As illustrated in Fig. 2.4C, the relative contributions of $EMG_{DIA,rms}$ and $EMG_{INT,rms}$ to $IND_{TOT,rms}$ decreased progressively, while the relative contributions of $EMG_{SCM,rms}$ and $EMG_{SCA,rms}$ to $IND_{TOT,rms}$ increased progressively with increasing $EILV_{\%IVC}$, with these changes becoming most notable in the transition from $EILV_{85\%}$ to $EILV_{95\%}$ (Table 2.4).

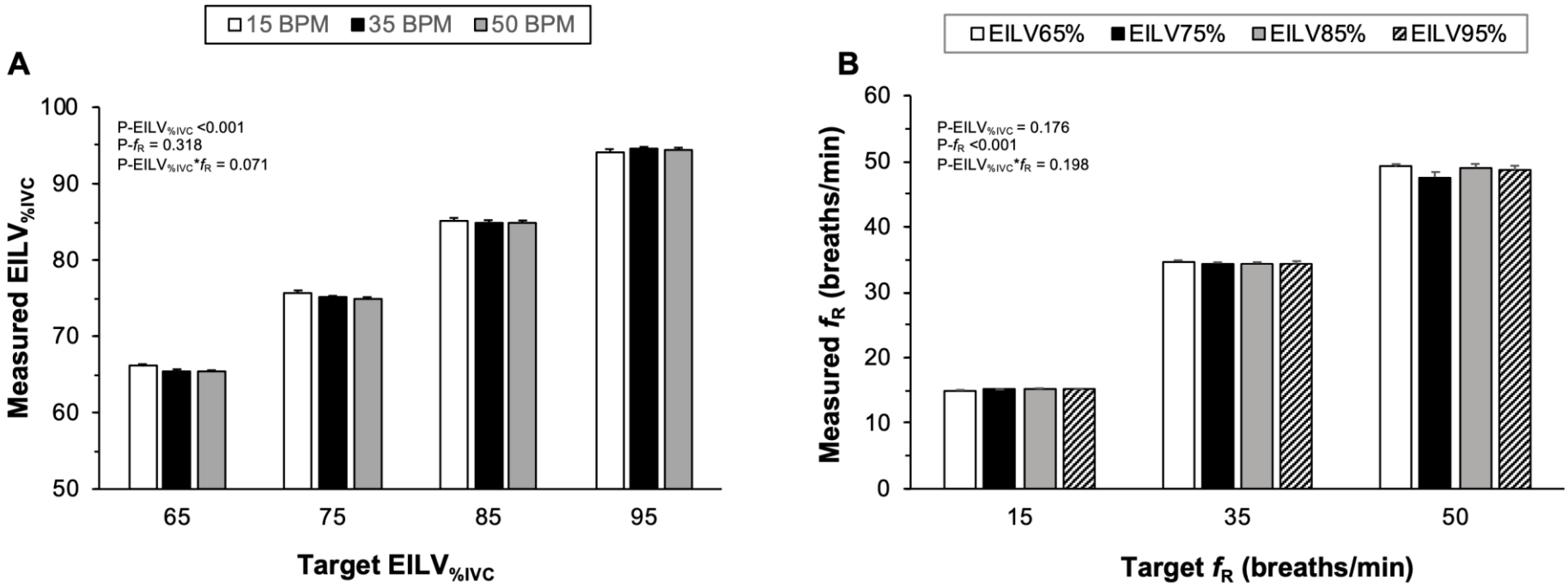

Figure 2.1. Measured versus targeted values of end-inspiratory lung volume and breathing frequency during breathing trials. Values are means ± SEM. ***Abbreviations***: $EILV_{\%IVC}$, end-inspiratory lung volume reference to inspired vital capacity; f_R, breathing frequency; 15 BPM, 35 BPM and 50 BPM, breathing frequency of 15, 35 and 50 breaths/min, respectively; EILV65%, EILV75%, EILV85% and EILV95%, end-inspiratory lung volume corresponding to 65%, 75%, 85% and 95% of inspired vital capacity, respectively.

Table 2.3. Effect of alterations in breathing frequency and end-inspiratory lung volume on physiological parameters

	f_R = 15 breaths/min				f_R = 35 breaths/min				f_R = 50 breaths/min				*p-value*		
	$EILV_{65\%}$	**$EILV_{75\%}$**	**$EILV_{85\%}$**	**$EILV_{95\%}$**	**$EILV_{65\%}$**	**$EILV_{75\%}$**	**$EILV_{85\%}$**	**$EILV_{95\%}$**	**$EILV_{65\%}$**	**$EILV_{75\%}$**	**$EILV_{85\%}$**	**$EILV_{95\%}$**	**$EILV_{\%IVC}$**	**f_R**	**$EILV_{\%IVC}$*f_R**
f_R (breaths/min)	15.0 ± 0.1	15.1 ± 0.1	15.2 ± 0.2	15.2 ± 0.1	34.8 ± 0.2	34.5 ± 0.1	34.4 ± 0.2	34.3 ± 0.5	49.2 ± 0.4	47.6 ± 0.8	49.0 ± 0.6	48.6 ± 0.7	0.176	<0.001	0.198
V_T (L)	1.93 ± 0.15	1.92 ± 0.15	1.89 ± 0.15	1.89 ± 0.14	0.82 ± 0.07	0.84 ± 0.06	0.83 ± 0.06	0.87 ± 0.07	0.60 ± 0.07	0.61 ± 0.05	0.61 ± 0.06	0.66 ± 0.06[a]	0.066	<0.001	0.034
V'_E (L/min)	29.0 ± 2.3	29.0 ± 2.3	28.7 ± 2.3	28.6 ± 2.0	28.5± 2.2	29.0 ± 2.2	28.6 ± 2.2	29.7 ± 2.6	29.2 ± 2.7	29.2 ± 2.5	29.9 ± 2.9	32.5 ± 2.8[a,b,c]	0.003	0.048	0.019
V'_E (% MVV)	16.4 ± 0.5	16.4 ± 0.5	16.2 ± 0.5	16.4 ± 0.7	16.1 ± 0.5	16.3 ± 0.5	16.2 ± 0.6	16.7 ± 0.4	16.4 ± 0.8	16.4 ± 0.4	16.6 ± 0.7	18.3 ± 0.8[a,b,c]	0.005	0.138	0.044
EILV (%IVC)	66.1 ± 0.3	75.6 ± 0.4	85.1 ± 0.4	94.1 ± 0.5	65.4 ± 0.3	75.0 ± 0.3	84.8 ± 0.4	94.6 ± 0.2	65.3 ± 0.3	74.9 ± 0.3	84.9 ± 0.3	94.4 ± 0.3	<0.001	0.318	0.071
EILV (L)	3.23 ± 0.22	3.70 ± 0.25	4.14 ± 0.28	4.59 ± 0.30	3.20 ± 0.23	3.67 ± 0.25	4.15 ± 0.28	4.62 ± 0.32	3.18 ± 0.22	3.67 ± 0.25	4.14 ± 0.28	4.61 ± 0.32	<0.001	0.571	0.089
IRV (L)	1.66 ± 0.11	1.20 ± 0.09	0.76 ± 0.06	0.31 ± 0.04	1.70 ± 0.11	1.23 ± 0.08	0.75 ± 0.06	0.28 ± 0.03	1.71 ± 0.12	1.23 ± 0.08	0.76 ± 0.05	0.29 ± 0.03	<0.001	0.571	0.089
EELV (%IVC)	28.6 ± 2.2	38.0 ± 2.3	47.6 ± 2.3	56.8 ± 2.3	46.3 ± 2.6	55.7 ± 2.4	65.8 ± 2.2	74.6 ± 2.6	52.9 ± 0.7	62.2 ± 0.8	72.1 ± 0.6	80.4 ± 0.9	<0.001	<0.001	0.873
EELV (L)	1.39 ± 0.12	1.85 ± 0.15	2.32 ± 0.18	2.77 ± 0.21	2.29 ± 0.22	2.75 ± 0.24	3.24 ± 0.27	3.67 ± 0.31	2.59 ± 0.18	3.05 ± 0.22	3.53 ± 0.24	3.94 ± 0.27	<0.001	<0.001	0.810
Heart rate (bpm)	76 ± 3	78 ± 4	77 ± 4	76 ± 3	74 ± 3	78 ± 3	74 ± 3	80 ± 3[a,b,c]	74 ± 3	74± 3	74 ± 3	83 ± 4[a,b,c]	<0.001	0.717	<0.001
$P_{ET}CO_2$ (mmHg)	23.8 ± 0.9	23.7 ± 0.8	23.5 ± 0.8	24.1 ± 0.7	24.9 ± 0.8	24.9 ± 0.8	24.7 ± 0.8	24.9 ± 0.9	24.4 ± 0.8	24.6 ± 0.6	24.9 ± 1.0	22.5 ± 1.2	0.683	0.389	0.052
SpO_2 (%)	98.1 ± 0.6	98.5 ± 0.3	98.4 ± 0.2	98.1± 0.3	98.5 ± 0.3	98.5 ± 0.2	98.1 ± 0.5	97.8 ± 0.4	98.3 ± 0.2	98.3 ± 0.4	98.0 ± 0.6	97.8 ± 0.4	0.247	0.710	0.889
T_I/T_{TOT} (%)	45 ± 1	45 ± 1	43 ± 2	41 ± 2	47 ± 1	46 ± 1	43 ± 3	40 ± 3	40 ± 3	40 ± 3	40 ± 3	43 ± 2	0.054	0.328	0.055
V_T/T_I (L/sec)	1.09 ± 0.09	1.10 ± 0.09	1.11 ± 0.08	1.22 ± 0.15	1.04 ± 0.09	1.07 ± 0.09	1.19 ± 0.11	1.29 ± 0.12	1.04 ± 0.09	1.07 ± 0.09	1.10 ± 0.11	1.28 ± 0.09	<0.001	0.865	0.644
$EMG_{di,rms}$ (mV)	64 ± 4	84 ± 5	117 ± 10	167 ± 13	67 ± 5	87 ± 7	118 ± 12	168 ± 14	65 ± 4	86 ± 7	120 ± 12	171 ± 14	<0.001	0.391	0.780
$EMG_{SCM,rms}$ (mV)	15 ± 3	20 ± 4	38 ± 6	114 ± 19	16 ± 3	19 ± 3	43 ± 9	153 ± 36	14 ± 2	21 ± 3	47 ± 10	143 ± 21	<0.001	0.244	0.361
$EMG_{SCA,rms}$ (mV)	30 ± 4	44 ± 6	71 ± 9	164 ± 24	28 ± 3	43 ± 5	69 ± 6	178 ± 34	32 ± 4	46 ± 7	74 ± 9	167 ± 24	<0.001	0.943	0.975
$EMG_{INT,rms}$ (mV)	12 ± 1	13 ± 1	17 ± 2	28 ± 4	11 ± 1	15 ± 2	20 ± 4	36 ± 7	11 ± 1	15 ± 2	19 ± 3	36 ± 6	<0.001	0.113	0.101
$IND_{TOT,rms}$ (mV)	121 ± 6	160 ± 10	243 ± 17	473 ± 34	121 ± 7	164 ± 11	251 ± 18	536 ± 57	122 ± 6	168 ± 9	260 ± 18	516 ± 40	<0.001	0.354	0.566
†Pdi,tidal (cmH_2O)	17.8 ± 1.4	20.5 ± 1.5	24.3 ± 2.2	37.2 ± 3.9	14.8 ± 1.2	19.8 ± 2.4	26.7 ± 3.2	40.0 ± 5.3	13.5 ± 1.2	15.3 ± 1.2	21.8 ± 2.8	33.7 ± 5.5	<0.001	0.117	0.879
†Pdi,inspir (cmH_2O)	35.1 ± 2.3	37.7 ± 2.2	42.4 ± 2.5	55.5 ± 4.3	31.5 ± 2.2	38.4 ± 3.3	45.0 ± 3.8	60.3 ± 5.9	32.4 ± 1.8	34.7 ± 1.6	40.4 ± 3.2	55.5 ± 6.5	<0.001	0.324	0.377
Pes,tidal (cmH_2O)	13.6 ± 0.9	14.4 ± 0.9	16.0 ± 1.0[a]	21.7 ± 2.3[a,b,c]	8.8 ± 0.6	9.3 ± 0.5	10.5 ± 0.8	14.4 ± 1.5[a,b,c]	7.3 ± 0.7	7.4 ± 0.5	8.7 ± 0.6	11.7± 0.9[a,b,c]	<0.001	<0.001	0.022
Pes,inspir (cmH_2O)	-17.9 ± 1.4	-20.7 ± 1.6	-24.3 ± 1.9	-31.2 ± 2.7	-17.0 ± 1.5	-20.2 ± 1.6	-23.1 ± 2.1	-29.9 ± 3.1	-16.6 ± 1.5	-19.1 ± 1.6	-22.3 ± 2.1	-27.9 ± 3.2	<0.001	0.019	0.669
†Pdi,inspir-$EMGdi_{,rms}$ ratio (cmH_2O/mV)	0.58 ± 0.04	0.49 ± 0.04	0.39 ± 0.04[a,b]	0.37 ± 0.03[a,b]	0.52 ± 0.04	0.48 ± 0.03	0.42 ± 0.04[a]	0.38 ± 0.03[a,b]	0.53 ± 0.04	0.44 ± 0.04[a]	0.38 ± 0.04[a,b]	0.38 ± 0.04[a,b]	<0.001	0.144	0.035
Pes,inspir-$IND_{TOT,rms}$ ratio (cmH_2O/mV)	-0.16 ± 0.01	-0.14 ± 0.01	-0.11 ± 0.01	-0.08 ± 0.01	-0.15 ± 0.01	-0.14 ± 0.01	-0.10 ± 0.01	-0.07 ± 0.01	-0.14 ± 0.01	-0.12 ± 0.01	-0.09 ± 0.01	-0.06 ± 0.01	<0.001	0.006	0.944

Values are means ± SEM. ***Abbreviations*:** f_R, breathing frequency; $EILV_{\%IVC}$, end-inspiratory lung volume referenced to inspired vital capacity; $EILV_{65\%}$, $EILV_{75\%}$, $EILV_{85\%}$ and $EILV_{95\%}$, end-inspiratory lung volume corresponding to 65%, 75%, 85% and 95% of inspired vital capacity, respectively; V_T, tidal volume; V'_E, minute ventilation; MVV, maximal voluntary ventilation; IVC, inspired vital capacity; EILV, end-inspiratory lung volume; IRV, inspiratory reserve volume; EELV, end-expiratory lung volume; $P_{ET}CO_2$, end-tidal PCO_2; SpO_2, blood O_2 saturation; T_I/T_{TOT}, inspiratory duty cycle; V_T/T_I, mean tidal inspiratory flow rate; $EMG_{DIA,rms}$, root mean square of the crural diaphragm electromyogram ; $EMG_{SCM,rms}$, root mean square of the sternocleidomastoid electromyogram; $EMG_{SCA,rms}$, root mean square of the scalene electromyogram; $EMG_{INT,rms}$, root mean square of the 7th external intercostal electromyogram; $IND_{TOT,rms}$, root mean square of total inspiratory neural drive calculated as the sum of $EMG_{DIA,rms}$, $EMG_{SCM,rms}$, $EMG_{SCA,rms}$ and $EMG_{INT,rms}$; Pdi,tidal, tidal transdiaphragmatic pressure swing; Pdi,inspir, peak tidal inspiratory transdiaphragmatic pressure; Pes,tidal, tidal esophageal pressure swing; Pes,inspir, peak tidal inspiratory esophageal pressure. †n=10. [a]p<0.05 versus $EILV_{65\%}$ within f_R condition; [b]p<0.05 versus $EILV_{75\%}$ within f_R condition; [c]p<0.05 versus $EILV_{85\%}$ within f_R condition.

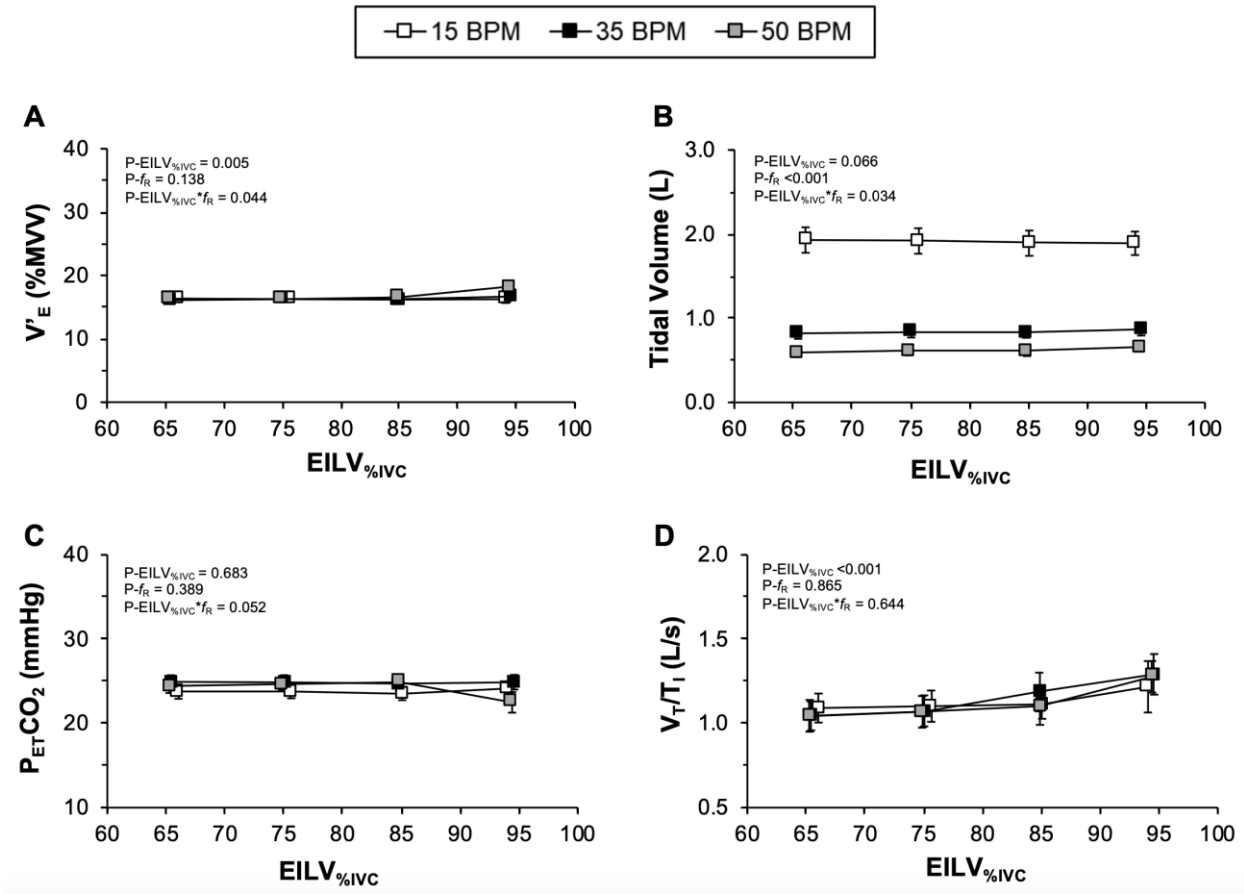

Figure 2.2. Pulmonary responses during breathing trials. Values are means ± SEM. ***Abbreviations***: 15 BPM, 35 BPM and 50 BPM, breathing frequency of 15, 35 and 50 breaths/min, respectively; $EILV_{\%IVC}$, end-inspiratory lung volume reference to inspired vital capacity; V'_E, minute ventilation; MVV, maximum voluntary ventilation; $P_{ET}CO_2$, end-tidal PCO_2; V_T/T_I, mean tidal inspiratory flow rate. Refer to Table 2.3 and text for results of pairwise comparisons.

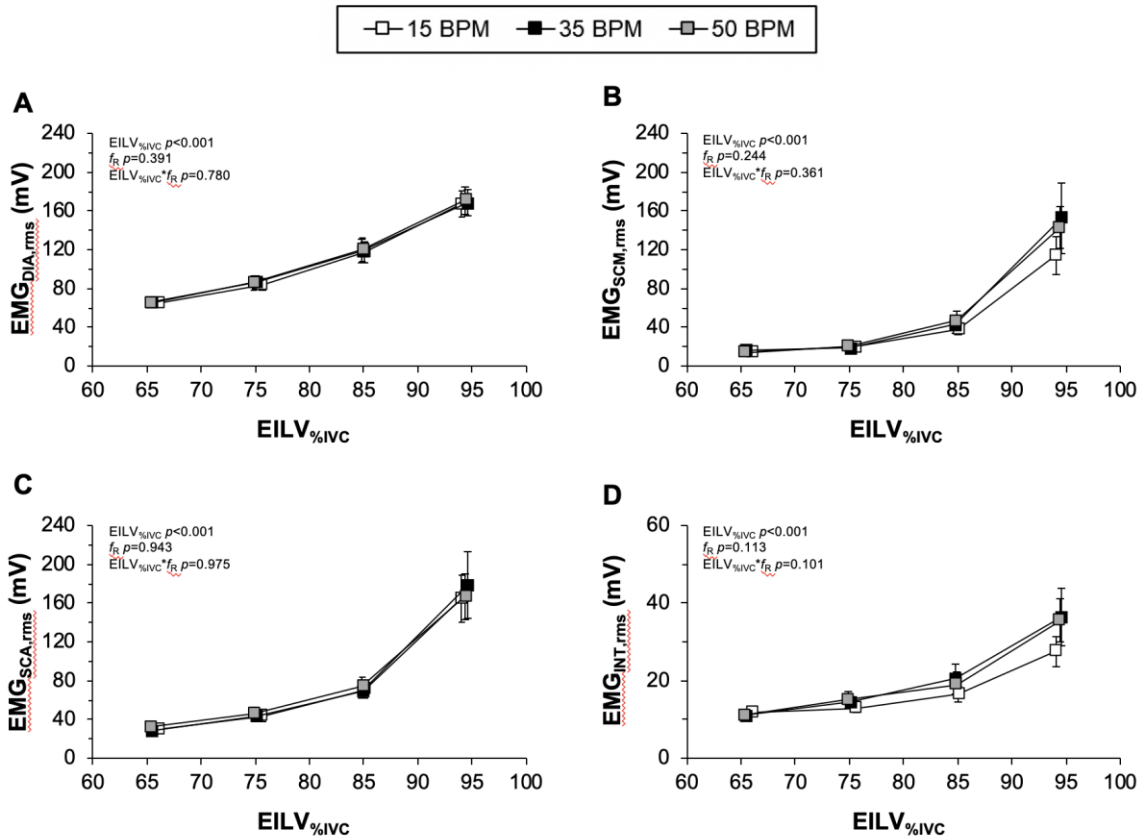

Figure 2.3. Inspiratory muscle EMG responses during breathing trials. Values are means ± SEM. ***Abbreviations***: 15 BPM, 35 BPM and 50 BPM, breathing frequency of 15, 35 and 50 breaths/min, respectively; $EILV_{\%IVC}$, end-inspiratory lung volume reference to inspired vital capacity; $EMG_{DIA,rms,}$ root mean square of the crural diaphragm electromyogram ; $EMG_{SCM,rms,}$ root mean square of the sternocleidomastoid electromyogram; $EMG_{SCA,rms,}$ root mean square of the scalene electromyogram; and $EMG_{INT,rms,}$ root mean square of the 7th external intercostal electromyogram.

Table 2.4. Effect of increasing end-inspiratory lung volume on the relative contribution of the diaphragm, sternocleidomastoid, scalene and 7th external intercostal muscles to an estimate of total inspiratory neural drive.

	$EILV_{65\%}$	$EILV_{75\%}$	$EILV_{85\%}$	$EILV_{95\%}$	*p-value*
$EMG_{DIA,rms}$ ($\%IND_{TOT,rms}$)	53.9 ± 2.5	52.5 ± 2.9	47.3 ± 2.8[a]	34.6 ± 2.9[a,b,c]	<0.001
$EMG_{SCM,rms}$ ($\%IND_{TOT,rms}$)	12.5 ± 2.0	12.3 ± 2.0	16.7 ± 2.5	26.0 ± 2.9[a,b,c]	<0.001
$EMG_{SCA,rms}$ ($\%IND_{TOT,rms}$)	24.3 ± 2.2	26.5 ± 2.8	28.7 ± 2.8[a]	32.8 ± 2.8[a,b,c]	<0.001
$EMG_{INT,rms}$ ($\%IND_{TOT,rms}$)	9.4 ± 0.7	8.7 ± 0.9	7.3 ± 0.8	6.6 ± 0.9[a]	<0.01

Values are means ± SEM. ***Abbreviations***: $EILV_{65\%}$, $EILV_{75\%}$, $EILV_{85\%}$ and $EILV_{95\%}$, end-inspiratory lung volume at 65%, 75%, 85% and 95% of inspired vital capacity, respectively; $EMG_{DIA,rms,}$ root mean square of the crural diaphragm eletromyogram; $EMG_{SCM,rms,}$ root mean square of the sternocleidomastoid electromyogram; $EMG_{SCA,rms,}$ root mean square of the scalene electromyogram; $EMG_{INT,rms,}$ root mean square of the 7th external intercostal electromyogram; $IND_{TOT,rms}$, root mean square of total inspiratory neural drive calculated as the sum of $EMG_{DIA,rms,}$ $EMG_{SCM,rms,}$ $EMG_{SCA,rms}$ and $EMG_{INT,rms}$. [a]$p<0.05$ versus $EILV_{65\%}$; [b]$p<0.05$ versus $EILV_{75\%}$; [c]$p<0.05$ versus $EILV_{85\%}$.

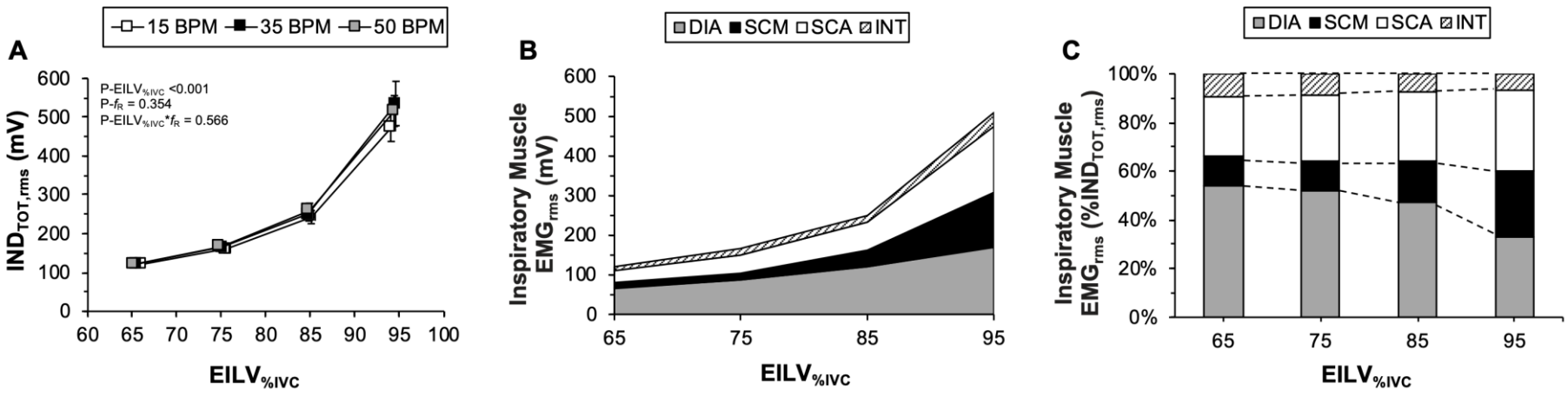

Figure 2.4. Inspiratory neural drive response during breathing trials. Values are means ± SEM (Panel A) and means (Panels B and C). ***Abbreviations***: 15 BPM, 35 BPM and 50 BPM, breathing frequency of 15, 35 and 50 breaths/min, respectively; DIA, crural diaphragm; SCM, sternocleidomastoid; SCA, scalene; INT, 7th external intercostal; $EILV_{\%IVC}$, end-inspiratory lung volume reference to inspired vital capacity; $IND_{TOT,rms}$, root mean square of total inspiratory neural drive calculated as the sum of the root mean square of the DIA, SCM, SCA and INT electromyogram; EMG_{rms}, root mean square of the electromyogram. Refer to Table 2.4 for summary of statistical results for the data presented in Panel C.

Both Pdi,tidal and Pdi,inspir (Fig. 2.5A) increased progressively with increasing $EILV_{\%IVC}$, independent of f_R or breathing pattern (Table 2.3). On average, Pes,tidal increased progressively with increasing $EILV_{\%IVC}$ and was significantly greater (i) at $EILV_{85\%}$ compared to $EILV_{65\%}$ within the $f_{R,15}$ condition and (ii) at $EILV_{95\%}$ compared to $EILV_{65\%}$, $EILV_{75\%}$ and $EILV_{85\%}$ within each of the three f_R conditions (Table 2.3). As illustrated in Fig. 2.5B, Pes,inspir decreased progressively with increasing $EILV_{\%IVC}$ within each of the f_R conditions and was consistently lower (by ~1-3 cmH_2O) at $f_{R,15}$ compared to $f_{R,50}$ across $EILV_{\%IVC}$ conditions (Table 2.3). Within each f_R condition, the ratio of Pdi,inspir to $EMG_{DIA,rms}$ decreased progressively from $EILV_{65\%}$ to $EILV_{85\%}$, with no further decrease thereafter (Fig. 2.5C, Table 2.3). As illustrated in Fig. 2.5D, the ratio of Pes,inspir to $IND_{TOT,rms}$ increased progressively with increasing $EILV_{\%IVC}$ within each of the f_R conditions and was consistently lower (by 0.02 cmH_2O/mV) at $f_{R,15}$ compared to $f_{R,50}$ across $EILV_{\%IVC}$ conditions (Table 2.3).

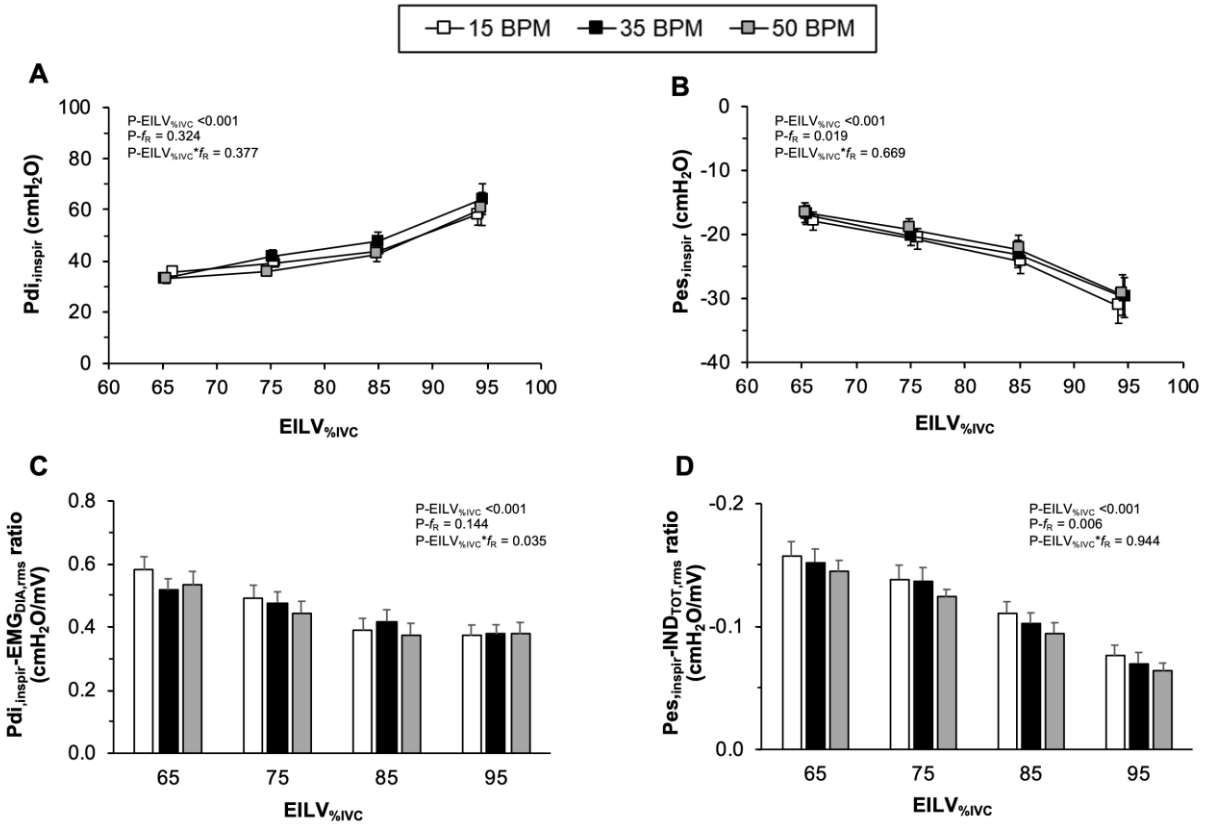

Figure 2.5. Inspiratory muscle pressure and neuromuscular coupling of the diaphragm/respiratory system responses during breathing trials. Values are means ± SEM. ***Abbreviations***: 15 BPM, 35 BPM and 50 BPM, breathing frequency of 15, 35 and 50 breaths/min, respectively; $EILV_{\%IVC}$, end-inspiratory lung volume reference to inspired vital capacity; Pdi,inspir, peak tidal inspiratory transdiaphragmatic pressure; Pes,inspir, peak tidal inspiratory esophageal pressure; EMG_{rms}, root mean square of the electromyogram; $EMG_{DIA,rms,}$ root mean square of the crural diaphragm electromyogram; $IND_{TOT,rms}$, root mean square of total inspiratory neural drive calculated as the sum of the root mean square of the crural diaphragm, sternocleidomastoid, scalene and 7th external intercostal electromyogram. Refer to Table 2.3 and text for results of pairwise comparisons.

2.5. DISCUSSION

The main findings of this study were that, in human subjects, independent of breathing pattern and EELV: (i) the level of central neural activation of the diaphragm and extra-diaphragmatic inspiratory muscles required to generate the intrathoracic pressures needed to support a constant V'_E increased as a function of increasing $EILV_{\%IVC}$; (ii) the relative contributions of the diaphragm and of the external intercostal muscles to an estimate of global central inspiratory neural drive decreased progressively, while the relative contributions of the sternocleidomastoid and scalene muscles to an estimate of global central inspiratory neural drive increased progressively with increasing $EILV_{\%IVC}$ at a constant V'_E; and (iii) neuromuscular coupling of the diaphragm and of the respiratory system deteriorated progressively with increasing $EILV_{\%IVC}$ at a constant V'_E.

Force-velocity and pressure-volume relationships predict that, for a given level of neural activation, the capacity of the inspiratory muscles to generate pressure falls with increasing inspiratory flow (increasing velocity of contraction) and/or increasing lung volume (decreasing inspiratory muscle length), respectively [45, 46, 64-67]. For example, Leblanc et al. [46] estimated that the capacity of the inspiratory muscles to generate negative esophageal pressure (i) decreased by 5% for each 1 L/sec increase in inspiratory flow and (ii) decreased by 1.7% for each 1% increase in lung volume above 55% of TLC. On the basis of these estimates, over the normal physiological range (i.e., from rest to peak exercise), the adverse effect of increasing inspiratory flow from ~1 L/sec at rest to ~5 L/sec at peak exercise on inspiratory muscle pressure generating capacity is proportionally less than that associated with increasing EILV from ~50% of TLC at rest to ~90% of TLC at peak exercise (i.e., ~20% vs. ~60% fall in inspiratory muscle pressure generating capacity).

The corollary of the above is that, in order for the diaphragm and extra-diaphragmatic inspiratory muscles to generate a given amount of intrathoracic pressure, their level of neural activation must rise with increasing inspiratory flow and/or increasing lung volume [3]. In our

study, V_T/T_I - an estimate of the velocity of inspiratory muscle contraction - ranged from ~1.0 to ~1.3 L/sec and was not significantly different across f_R conditions within any given $EILV_{\%IVC}$ condition, but was significantly higher at $EILV_{95\%}$ compared to $EILV_{65\%}$, $EILV_{75\%}$ and $EILV_{85\%}$ within each of the f_R conditions. Thus, while a progressive increase in V_T/T_I cannot account for the progressive rise in inspiratory muscle EMG activity from $EILV_{65\%}$ to $EILV_{85\%}$, it is possible that the marked increase in neural activation of the diaphragm and of the extra-diaphragmatic inspiratory muscles in the transition from $EILV_{85\%}$ to $EILV_{95\%}$ reflected not only the consequences of breathing on the uppermost extreme of the respiratory systems' sigmoid pressure-volume curve (*see below*), but also the influence of increased velocity of inspiratory muscle contraction on inspiratory muscle pressure generating capacity. However, the absolute differences in V_T/T_I whilst breathing at $EILV_{95\%}$ compared to $EILV_{65\%}$, $EILV_{75\%}$ and $EILV_{85\%}$ were very small (0.10-0.28 L/sec) and would be expected to decrease inspiratory muscle pressure generating capacity by just 0.5-1.5% [46]. Thus, it seems unlikely that these small but statistically significant differences in V_T/T_I contributed meaningfully to the notable rise in $EMG_{DIA,rms}$, $EMG_{SCM,rms}$, $EMG_{SCA,rms}$ and $EMG_{INT,rms}$ in the transition from breathing at $EILV_{85\%}$ to $EILV_{95\%}$. Indeed, Beck et al. [64] reported no change in $EMG_{DIA,rms}$ when healthy participants breathed from functional residual capacity (FRC) to TLC at inspiratory flow rates between 0.1 to 1.4 L/sec. Washino et al. [2] similarly observed no change in EMG_{SCM} or EMG_{SCA} when healthy participants breathed from 20% to 60% of FVC at inspiratory flow rates ≤40% of their peak inspiratory flow rate (equivalent to inspiratory flow rates of ≤3.37 L/sec based on a reported mean peak inspiratory flow rate of 8.43 L/sec).

In our study, participants increased their EILV from 65% to 95% of IVC at each of three different breathing patterns designed to maintain a constant V'_E. As EILV increases towards TLC (or IRV decreases towards 0 L), expansion of V_T is forced to occur on the uppermost (alinear)

extreme of the respiratory systems' sigmoid pressure-volume curve where there is both an increased demand (secondary to decreased lung and chest wall compliance with attendant elastic loading) and decreased capacity (secondary to shortening of the diaphragm and extra-diaphragmatic inspiratory muscles) of the inspiratory muscles to generate pressure. It follows that when our participants increased their EILV from 65% to 95% of IVC (and decreased their IRV from ~1.7 to ~0.3 L), compensatory (reflex) increases in central inspiratory neural drive to the diaphragm and extra-diaphragmatic inspiratory muscles were required to generate the intrathoracic pressures needed to support a constant V'_E. As illustrated in Figs. 2.5C and 2.5D, the magnitudes of increase in $EMG_{DIA,rms}$ and $IND_{TOT,rms}$ with increasing $EILV_{\%IVC}$ were proportionally greater than the respective magnitudes of increase in Pdi,inspir and decrease in Pes,inspir at constant V'_E, independent of breathing pattern and EELV. These changes in Pdi,inspir-$EMG_{DIA,rms}$ and Pes,inspir-$IND_{TOT,rms}$ relationships were interpreted respectively as evidence of progressive neuromuscular uncoupling of the diaphragm and of the respiratory system as (i) load-capacity relationships of the diaphragm and extra-diaphragmatic inspiratory muscles deteriorated with increasing $EILV_{\%IVC}$ or decreasing IRV and (ii) V_T expansion transitioned from the linear (compliant) to the alinear (non-compliant) portion of the respiratory systems' sigmoid pressure-volume curve.

Interestingly, at any given $EILV_{\%IVC}$, the level of diaphragm and extra-diaphragmatic inspiratory muscle EMG activity needed to support a relatively constant V'_E, Pdi,inspir and Pdi,inspir was unaffected by differences in breathing pattern and EELV. On the basis of these observations, we drew the following conclusions. First, it matters more *where* an individual breathes relative to TLC than *how* they breathe with respect to the f_R and V_T they adopt in determining the level of central inspiratory neural drive needed to support a given V'_E and amount of intrathoracic pressure development. Second, EELV is important in determining the level of

central inspiratory neural drive needed to support a given V'_E and amount of intrathoracic pressure development through its effect on EILV (or IRV) and, by extension, the load-capacity relationship of the diaphragm and extra-diaphragmatic inspiratory muscles [46]. In other words, at any given level of V_T expansion, a decrease in EELV (such as occurs in the transition from rest to exercise in healthy adults [68, 69]) will decrease the level of central inspiratory neural drive needed to support a given V'_E by decreasing EILV (or increasing IRV) and optimizing load-capacity relationships of the diaphragm and extra-diaphragmatic inspiratory muscles. Alternatively, at any given level of V_T expansion, an increase in EELV (such as occurs in the transition from rest to exercise in people with chronic obstructive pulmonary disease [70]) will increase the level of central inspiratory neural drive needed to support a given V'_E by increasing EILV (or decreasing IRV) and compromising load-capacity relationships of the diaphragm and extra-diaphragmatic inspiratory muscles.

In this study, differences were observed in the neural activation (recruitment) pattern of the diaphragm and of the extra-diaphragmatic inspiratory muscles with increasing $EILV_{\%IVC}$ at constant V'_E, independent of breathing pattern and EELV. Specifically, although $EMG_{DIA,rms}$, $EMG_{SCM,rms}$, $EMG_{SCA,rms}$ and $EMG_{INT,rms}$ all increased with increasing $EILV_{\%IVC}$, the relative contributions of $EMG_{DIA,rms}$ and $EMG_{INT,rms}$ to $IND_{TOT,rms}$ progressively decreased, while the relative contributions of $EMG_{SCM,rms}$ and $EMG_{SCA,rms}$ to $IND_{TOT,rms}$ progressively increased with increasing $EILV_{\%IVC}$. As illustrated in Figs. 2.4B and 2.4C, the magnitudes of these changes were most prominent in the transition from $EILV_{85\%}$ to $EILV_{95\%}$, when IRV declined from ~0.75 L to a critically low value of ~0.30 L (which is well below the O'Donnell threshold [71]) and V_T was forced to expand on the uppermost (alinear) extreme of the respiratory systems' sigmoid pressure-volume curve, as indicated by a notable rise in Pdi,inspir and fall in Pes,inspir between $EILV_{85\%}$ and $EILV_{95\%}$. On the basis of these observations, we contend that, as EILV increased toward TLC

(or IRV decreased toward 0 L) and the diaphragm shortened, weakened and became a less effective pressure generator [45], there was preferential recruitment of the sternocleidomastoid and scalene muscles, which we assume had relatively greater inspiratory mechanical advantages [67, 72], to (i) elevate the rib cage, (ii) generate the intrathoracic pressures needed to maintain a constant V'_E and (ii) prevent excessive loading, weakening, neuromuscular uncoupling and fatigue of the diaphragm. This interpretation is supported by differences in the effect of $EILV_{\%IVC}$ on Pdi,inspir-$EMG_{DIA,rms}$ and Pes,inspir-$IND_{TOT,rms}$ relationships, as illustrated in Figs. 2.4B and 2.4C, respectively. Specifically, Pdi,inspir-$EMG_{DIA,rms}$ relationships worsened progressively from $EILV_{65\%}$ to $EILV_{85\%}$, with no further change thereafter. This is in contrast to Pes,inspir-$IND_{TOT,rms}$ relationships, which deteriorated progressively from $EILV_{65\%}$ to $EILV_{95\%}$. Our interpretation is further supported by the results of (i) Raper et al. [53] who showed that both EMG_{SCA} and EMG_{SCM} activity increased progressively (albeit in different proportions and with different time courses of change) with increasing lung volume until 100% vital capacity was approached, at which point EMG_{SCA} and EMG_{SCM} increased abruptly; (ii) Ramsook et al. [54] who observed a precipitous rise in both EMG_{SCA} and EMG_{SCM} starting at an EILV of ~80% of TLC during maximal incremental cycle exercise testing in healthy adults; (iii) Mitchell et al. [73] who showed that both EMG_{SCM} and EMG_{SCA} were higher in the setting of a lower IRV throughout high-intensity constant-load cycle exercise testing in healthy women vs. men; and (iv) Hudson et al. [74] who found that the mechanically advantageous effects associated with adopting an upside-down compared to upright posture (e.g., decreased EELV and EILV, increased intra-abdominal pressure, reduced abdominal wall compliance, increased diaphragm length and zone of apposition) improved neuromuscular coupling of the diaphragm (as evidenced by increased Pdi,tidal-EMG_{DIA} relationships) and decreased EMG_{SCA} by ~50% despite little and no change in V'_E and V_T, respectively, during quiet breathing in healthy adults.

The observed relationship between $EILV_{\%IVC}$ and each of $EMG_{DIA,rms}$, $EMG_{SCM,rms}$, $EMG_{SCA,rms}$ and $EMG_{INT,rms}$ could not be explained by increased respiratory chemoreflex stimulation since both $P_{ET}CO_2$ and SpO_2 were not significantly different across $EILV_{\%IVC}$ trials. In fact, mean $P_{ET}CO_2$ values were ~22-25 mmHg (hypocapnic) across all trials, suggesting that inspiratory muscle EMG-$EILV_{\%IVC}$ relationships may have may have been attenuated by relatively reduced respiratory chemoreflex activity.

2.5.1. Methodological considerations. Advantages and disadvantages of using esophageal and transcutaneous EMG electrodes to assess for changes in central inspiratory neural drive have been discussed elsewhere [60, 75, 76].

Given the within-subject design of this study, all EMG data were reported in absolute values, which is appropriate for intraindividual comparisons [75, 77], rather than as a percentage of maximal voluntary EMG, which is recommended for interindividual comparisons [75, 77, 78].

The esophageal electrode used in our study records EMG activity from a portion of the crural diaphragm. Nguyen et al. [79] recently reported that (i) the increase in inspiratory EMG activity from quiet breathing was proportionally greater in the costal than in the crural diaphragm of human subjects during voluntary and involuntary increases in central inspiratory neural drive and (ii) the source of increased central inspiratory neural drive (voluntary or involuntary) did not affect the proportion of costal to crural diaphragm EMG activity. On the basis of these observations, it is reasonable to make the following assumptions. First, our measures of $EMG_{DIA,rms}$ underestimated the effect of increasing $EILV_{\%IVC}$ on global diaphragm activation, but that this underestimation would not have altered the interpretation of our results since costal and crural diaphragm EMG activity increased linearly and simultaneously (albeit in different proportions) with voluntary or involuntary increases of central inspiratory neural drive [79].

Second, the observed effect of increasing $EILV_{\%IVC}$ on $EMG_{DIA,rms}$ does not depend on the source (voluntary or involuntary) of increased central inspiratory neural drive. Thus, the $EMG_{DIA,rms}$ results of our study that involved voluntary control of breathing, should apply to conditions associated with involuntary control of breathing (e.g., exercise, sleep, hypercapnia, hypoxia). Based on the results of Hudson et al. [80], however, it is possible that the effect of $EILV_{\%IVC}$ on $EMG_{SCM,rms}$, $EMG_{SCA,rms}$ and $EMG_{INT,rms}$ may depend on the source (voluntary or involuntary) of increased central inspiratory neural drive. Additional research is needed in this regard.

It is possible that unmeasured differences in chest wall configuration across trials could have affected measurement of $EMG_{DIA,rms}$ independently of changes in $EILV_{\%IVC}$ by affecting (i) the length of the crural diaphragm and (ii) the distance between the esophageal electrode and the crus of the diaphragm (i.e., muscle-to-electrode distance). However, the esophageal electrode used in our study has an interelectrode distance of 3.4 cm within each of the 5 consecutive recording pairs that, once optimally positioned and fixed externally to the nose, covers the span of movement of the crural diaphragm associated with changes in (i) lung volume from residual volume to FRC plus 2 L [60, 81] and (ii) V_T from <1 L to ≥3 L [82]. Possible changes in muscle-to-electrode distance with movement of the crural diaphragm across trials were further accounted for during analysis by selecting the largest $EMG_{DIA,rms}$ value from any one of the 5 electrode recording pairs. For all of these reasons, we are confident that the esophageal electrode used in our study provided reliable recording of $EMG_{DIA,rms}$ across trials.

While not directly assessed, it is possible that the skin surface electrodes used to record $EMG_{INT,rms}$ may have changed position and come to overlie the ribs with changes in $EILV_{\%IVC}$ [45] and/or breathing pattern. While this may have compromised the quality of the EMG_{INT} signal obtained, we nevertheless observed a similar pattern of change in $EMG_{INT,rms}$ with increasing $EILV_{\%IVC}$ as we did for $EMG_{DIA,rms}$, $EMG_{SCM,rms}$ and $EMG_{SCA,rms}$.

Transcutaneous measures of $EMG_{SCA,rms}$ and $EMG_{SCM,rms}$ are susceptible to crosstalk contamination. Visual inspection of EMG_{SCM} and EMG_{SCA} during maximum voluntary contralateral rotations of the head against resistance prior to the start of breathing trials confirmed a marked increase EMG_{SCM} without a corresponding change EMG_{SCA} in each participant. While this mitigates the likelihood of crosstalk contamination of $EMG_{SCA,rms}$ from $EMG_{SCM,rms}$, we cannot rule out the possibility of crosstalk contamination of $EMG_{SCM,rms}$ from $EMG_{SCA,rms}$.

It could be argued that the observed effect of increasing $EILV_{\%IVC}$ on $EMG_{DIA,rms}$ and Pdi,inspir-$EMG_{DIA,rms}$ relationships may be due, at least in part, to diaphragm fatigue caused by participants performing repeated breathing trials under conditions of both increased demand and decreased capacity of the diaphragm to generate pressure and maintain V'_E. Although objective assessments of diaphragm fatigue were not made, this phenomenon was unlikely to have developed because breathing trials were short (30-sec), interspersed by ≥1-min of rest, randomized to order, and performed at a level of V'_E corresponding to just 15% of each participants MVV. Furthermore, Ward et al. [83] found that development of diaphragm fatigue was accompanied by a progressive decline in EMG_{DIA} at constant f_R, V_T, V_T/T_I and T_I/T_{TOT}, whereas Luo et al. [82] observed no effect of diaphragm fatigue on $EMG_{DIA,rms}$-V'_E and $EMG_{DIA,rms}$-V_T relationships (slopes) during CO_2 rebreathing. In contrast to the results of Ward et al. [83] and Luo et al. [82], we found that $EMG_{DIA,rms}$ increased progressively with increasing $EILV_{\%IVC}$ at constant V'_E, independent of f_R, V_T, V_T/T_I and T_I/T_{TOT}. For all of these reasons, it is unlikely that ostensible diaphragm fatigue influenced our results and their interpretation.

2.5.2. Physiological and clinical implications. The results of our study suggest that between-group differences in the behaviour of dynamic EILV (or IRV) – not breathing pattern and/or EELV – are mechanistically linked to the exaggerated EMG_{DIA}-V'_E relationship observed during exercise in

(i) people with compared to without chronic obstructive or restrictive pulmonary disease [27, 32, 38, 56]; (ii) the presence compared to absence of a mild restrictive lung deficit *via* external thoracic restriction [40]; (iii) women compared to men [31, 33]; and (iv) older compared to younger adults [31]. The corollary of this is that, in people with chronic obstructive pulmonary disease, improved EMG_{DIA}-V'_E relationships during exercise following lung volume reduction surgery [84] or bronchodilator therapy [85] likely reflect, at least in part, concurrent improvement in the behaviour of dynamic EILV (or IRV).

As reviewed in detail elsewhere [86], both esophageal and transcutaneous electrode-derived measures of inspiratory muscle EMG activity have emerged as biomarkers of exertional breathlessness in people with chronic obstructive or restrictive pulmonary disease [15, 27, 32, 38, 55, 87, 88]. The results of our study provide indirect support of the hypothesis that, compared to healthy controls, the higher intensity ratings of exertional breathlessness reported by people with chronic obstructive or restrictive pulmonary disease is mechanistically linked to the awareness of proportionally greater central inspiratory neural drive needed to compensate for established pathophysiological abnormalities in the behaviour of dynamic EILV (or IRV).

2.5.3. Conclusion. The results of this study are unique and revealed a critical mechanistic role of EILV (or IRV) in determining the level of central inspiratory neural drive to the diaphragm and extra-diaphragmatic inspiratory muscles required to generate the intrathoracic pressures needed to support a given level of V'_E, independent of breathing pattern and EELV. These findings have potentially important implications for the assessment and interpretation of respiratory muscle function and activation under a variety of conditions (e.g., rest, sleep, exercise, medical intervention) in health and disease.

REFERENCES

1. Hussain, S., R. Pardy, and J. Dempsey, *Mechanical impedance as determinant of inspiratory neural drive during exercise in humans.* Journal of Applied Physiology, 1985. **59**(2): p. 365-375.
2. Washino, S., H. Kanehisa, and Y. Yoshitake, *Neck inspiratory muscle activation patterns during well-controlled inspiration.* European journal of applied physiology, 2017. **117**(10): p. 2085-2097.
3. Beck, J., et al., *Crural diaphragm activation during dynamic contractions at various inspiratory flow rates.* Journal of Applied Physiology, 1998. **85**(2): p. 451-458.
4. Aubier, M., T. Trippenbach, and C. Roussos, *Respiratory muscle fatigue during cardiogenic shock.* Journal of Applied Physiology, 1981. **51**(2): p. 499-508.
5. Hussain, S., G. Simkus, and C. Roussos, *Respiratory muscle fatigue: a cause of ventilatory failure in septic shock.* Journal of applied physiology, 1985. **58**(6): p. 2033-2040.
6. Lourenco, R., et al., *Nervous output from the respiratory center during obstructed breathing.* Journal of applied physiology, 1966. **21**(2): p. 527-533.
7. Luo, Y., et al., *Neural respiratory drive during apnoeic events in obstructive sleep apnoea.* European Respiratory Journal, 2008. **31**(3): p. 650-657.
8. Steier, J., et al., *Sleep-disordered breathing in unilateral diaphragm paralysis or severe weakness.* European Respiratory Journal, 2008. **32**(6): p. 1479-1487.
9. Luo, Y.-M., et al., *Distinguishing obstructive from central sleep apnea events: diaphragm electromyogram and esophageal pressure compared.* Chest, 2009. **135**(5): p. 1133-1141.
10. Luo, Y., et al., *Neural drive during continuous positive airway pressure (CPAP) and pressure relief CPAP.* Sleep medicine, 2009. **10**(7): p. 731-738.
11. Tang, J., Y. Lu, and Y. Luo, *Respiratory effort assessed by surface diaphragm EMG in patients with sleep apnea.* Zhonghua jie he he hu xi za zhi= Zhonghua jiehe he huxi zazhi= Chinese journal of tuberculosis and respiratory diseases, 2009. **32**(10): p. 732-735.
12. Steier, J., et al., *Increased load on the respiratory muscles in obstructive sleep apnea.* Respiratory physiology & neurobiology, 2010. **171**(1): p. 54-60.
13. Xu, J., et al., *Neural respiratory drive and nocturnal hypoventilation in patients with chronic obstructive pulmonary disease.* Zhonghua yi xue za zhi, 2013. **93**(6): p. 411-414.
14. Luo, Y.-M., et al., *Neural respiratory drive and ventilation in patients with chronic obstructive pulmonary disease during sleep.* American journal of respiratory and critical care medicine, 2014. **190**(2): p. 227-229.
15. Jolley, C.J., et al., *Neural respiratory drive and breathlessness in COPD.* European Respiratory Journal, 2015. **45**(2): p. 355-364.
16. Xiao, S.-C., et al., *Neural respiratory drive and arousal in patients with obstructive sleep apnea hypopnea.* Sleep, 2015. **38**(6): p. 941-949.
17. He, B.-T., et al., *Coexistence of OSA may compensate for sleep related reduction in neural respiratory drive in patients with COPD.* Thorax, 2017. **72**(3): p. 256-262.
18. Mally, P.V., et al., *Neural breathing pattern and patient-ventilator interaction during neurally adjusted ventilatory assist and conventional ventilation in newborns.* Pediatric Critical Care Medicine, 2018. **19**(1): p. 48-55.
19. Liu, L., et al., *Neuroventilatory efficiency and extubation readiness in critically ill patients.* Critical Care, 2012. **16**(4): p. R143.
20. Grasselli, G., et al., *Assessment of patient–ventilator breath contribution during neurally adjusted ventilatory assist.* Intensive care medicine, 2012. **38**(7): p. 1224-1232.
21. Sinderby, C. and J. Beck, *Neurally adjusted ventilatory assist in non-invasive ventilation.* Minerva anestesiologica, 2013. **79**(8): p. 915-925.

22. Sinderby, C. and J. Beck, *Neurally adjusted ventilatory assist: first indications of clinical outcomes.* Journal of critical care, 2014. **29**(4): p. 666.
23. Liu, L., et al., *Assessment of patient-ventilator breath contribution during neurally adjusted ventilatory assist in patients with acute respiratory failure.* Critical Care, 2015. **19**(1): p. 43.
24. Beck, J., Y. Liu, and C. Sinderby, *Noninvasive Neurally Adjusted Ventilatory Assist (NIV-NAVA) in Children and Adults*, in *Noninvasive Mechanical Ventilation*. 2016, Springer. p. 145-152.
25. Sinderby, C. and J. Beck, *Proportional assist ventilation and neurally adjusted ventilatory assist—better approaches to patient ventilator synchrony?* Clinics in chest medicine, 2008. **29**(2): p. 329-342.
26. Sinderby, C., et al., *Inspiratory muscle unloading by neurally adjusted ventilatory assist during maximal inspiratory efforts in healthy subjects.* Chest, 2007. **131**(3): p. 711-717.
27. Faisal, A., et al., *Common mechanisms of dyspnea in chronic interstitial and obstructive lung disorders.* American journal of respiratory and critical care medicine, 2016. **193**(3): p. 299-309.
28. Guenette, J.A., et al., *Neuromechanical uncoupling of the respiratory system during exercise in patients with mild COPD.* European Respiratory Journal, 2013. **42**(Suppl 57): p. P1833.
29. Jensen, D., et al., *Effects of dead space loading on neuro-muscular and neuro-ventilatory coupling of the respiratory system during exercise in healthy adults: implications for dyspnea and exercise tolerance.* Respiratory physiology & neurobiology, 2011. **179**(2-3): p. 219-226.
30. Jolley, C.J., et al., *Neural respiratory drive in healthy subjects and in COPD.* European Respiratory Journal, 2009. **33**(2): p. 289-297.
31. Molgat-Seon, Y., et al., *Effects of age and sex on inspiratory muscle activation patterns during exercise.* Medicine & Science in Sports & Exercise, 2018. **50**(9), 1882-1891.
32. Reilly, C.C., et al., *Neural respiratory drive, pulmonary mechanics and breathlessness in patients with cystic fibrosis.* Thorax, 2011. **66**(3): p. 240-246.
33. Schaeffer, M.R., et al., *Physiological mechanisms of sex differences in exertional dyspnoea: role of neural respiratory motor drive.* Experimental physiology, 2014. **99**(2): p. 427-441.
34. Sinderby, C., et al., *Diaphragm activation during exercise in chronic obstructive pulmonary disease.* American Journal of Respiratory and Critical Care Medicine, 2001. **163**(7): p. 1637-1641.
35. Wilkinson-Maitland, C., et al., *Exertional dyspnea relief following bronchodilation in COPD: Role of neural respiratory drive*. European Respiratory Journal Sep 2015, **46** (suppl 59) PA4626
36. Ciavaglia, C.E., et al., *Neuromuscular dissociation of the diaphragm is more pronounced during treadmill exercise compared with cycle exercise in obese COPD patients.* European Respiratory Journal, 2014. **44**(Suppl 58): p. P3530.
37. Luo, Y. and J. Moxham, *Measurement of neural respiratory drive in patients with COPD.* Respiratory physiology & neurobiology, 2005. **146**(2-3): p. 165-174.
38. Guenette, J.A., et al., *Mechanisms of exercise intolerance in global initiative for chronic obstructive lung disease grade 1 COPD.* European Respiratory Journal, 2014. **44**(5): p. 1177-1187.
39. Qin, Y.-Y., et al., *Efficiency of neural drive during exercise in patients with COPD and healthy subjects.* Chest, 2010. **138**(6): p. 1309-1315.

40. Mendonca, C.T., et al., *Physiological mechanisms of dyspnea during exercise with external thoracic restriction: role of increased neural respiratory drive.* Journal of Applied Physiology, 2014. **116**(5): p. 570-581.
41. Hill, A.V., *The heat of shortening and the dynamic constants of muscle.* Proceedings of the Royal Society of London. Series B-Biological Sciences, 1938. **126**(843): p. 136-195.
42. Martini, F.H., J.L. Nath, and E.F. Bartholomew, *Fundamentals of Anatomy and Physiology.. Glenview, IL*. 2015, Pearson Education.
43. Braun, N., N.S. Arora, and D.F. Rochester, *Force-length relationship of the normal human diaphragm.* Journal of Applied Physiology, 1982. **53**(2): p. 405-412.
44. Loring, S.H., J. Mead, and N.T. Griscom, *Dependence of diaphragmatic length on lung volume and thoracoabdominal configuration.* Journal of Applied Physiology, 1985. **59**(6): p. 1961-1970.
45. Smith, J. and F. Bellemare, *Effect of lung volume on in vivo contraction characteristics of human diaphragm.* Journal of Applied Physiology, 1987. **62**(5): p. 1893-1900.
46. Leblanc, P., et al., *Inspiratory muscles during exercise: a problem of supply and demand.* Journal of Applied Physiology, 1988. **64**(6): p. 2482-2489.
47. Rahn, H., et al., *The pressure-volume diagram of the thorax and lung.* American Journal of Physiology-Legacy Content, 1946. **146**(2): p. 161-178.
48. Brizendine, R.K., et al., *Velocities of unloaded muscle filaments are not limited by drag forces imposed by myosin cross-bridges.* Proceedings of the National Academy of Sciences, 2015. **112**(36): p. 11235-11240.
49. Agostoni, E. and W. Fenn, *Velocity of muscle shortening as a limiting factor in respiratory air flow.* Journal of Applied Physiology, 1960. **15**(3): p. 349-353.
50. Grimby, G., B. Saltin, and L. Wilhelmsen, *Pulmonary flow-volume and pressure-volume relationship during submaximal and maximal exercise in young well-trained men.* Bulletin de physio-pathologie respiratoire, 1971. **7**(1): p. 157.
51. Murphy, P.B., et al., *Neural respiratory drive as a physiological biomarker to monitor change during acute exacerbations of COPD.* Thorax, 2011. **66**(7): p. 602-608.
52. Reilly, C.C., et al., *Neural respiratory drive measured during inspiratory threshold loading and acute hypercapnia in healthy individuals.* Experimental physiology, 2013. **98**(7): p. 1190-1198.
53. Raper, A.J., et al., *Scalene and sternomastoid muscle function.* Journal of Applied Physiology, 1966. **21**(2): p. 497-502.
54. Ramsook, A.H., et al., *Effects of inspiratory muscle training on respiratory muscle electromyography and dyspnea during exercise in healthy men.* Journal of Applied Physiology, 2017. **122**(5): p. 1267-1275.
55. Schaeffer, M.R., et al., *Neurophysiological mechanisms of exertional dyspnoea in fibrotic interstitial lung disease.* Eur Respir J, 2018. **51**(1).
56. Qin, Y.Y., et al., *Efficiency of neural drive during exercise in patients with COPD and healthy subjects.* Chest, 2010. **138**(6): p. 1309-15.
57. Quanjer, P.H., et al., *Multi-ethnic reference values for spirometry for the 3-95-yr age range: the global lung function 2012 equations.* Eur Respir J, 2012. **40**(6): p. 1324-43.
58. Johnson, B.D., et al., *Emerging concepts in the evaluation of ventilatory limitation during exercise: the exercise tidal flow-volume loop.* Chest, 1999. **116**(2): p. 488-503.
59. Luo, Y., et al., *Neural respiratory drive in patients with COPD during exercise tests.* Respiration, 2011. **81**(4): p. 294-301.
60. Luo, Y.M., J. Moxham, and M.I. Polkey, *Diaphragm electromyography using an oesophageal catheter: current concepts.* Clinical science, 2008. **115**(8): p. 233-244.

61. Hermens, H.J., et al., *Development of recommendations for SEMG sensors and sensor placement procedures.* Journal of electromyography and Kinesiology, 2000. **10**(5): p. 361-374.
62. Cabral, E.E., et al., *Surface electromyography (sEMG) of extradiaphragm respiratory muscles in healthy subjects: A systematic review.* Journal of Electromyography and Kinesiology, 2018. **42**: p. 123-135.
63. Guenette, J.A., et al., *Blood flow index using near-infrared spectroscopy and indocyanine green as a minimally invasive tool to assess respiratory muscle blood flow in humans.* American Journal of Physiology-Regulatory, Integrative and Comparative Physiology, 2011. **300**(4): p. R984-R992.
64. Beck, J., et al., *Effects of lung volume on diaphragm EMG signal strength during voluntary contractions.* J Appl Physiol (1985), 1998. **85**(3): p. 1123-34.
65. Laghi, F., M.J. Harrison, and M.J. Tobin, *Comparison of magnetic and electrical phrenic nerve stimulation in assessment of diaphragmatic contractility.* Journal of Applied Physiology, 1996. **80**(5): p. 1731-1742.
66. Hyatt, R.E. and R.E. Flath, *Relationship of air flow to pressure during maximal respiratory effort in man.* Journal of Applied Physiology, 1966. **21**(2): p. 477-482.
67. Hudson, A.L., S.C. Gandevia, and J.E. Butler, *The effect of lung volume on the co-ordinated recruitment of scalene and sternomastoid muscles in humans.* The Journal of physiology, 2007. **584**(1): p. 261-270.
68. Sheel, A.W. and L.M. Romer, *Ventilation and respiratory mechanics.* Comprehensive Physiology, 2012. **2**(2): p. 1093-142.
69. Jensen, D., D. Ofir, and D.E. O'Donnell, *Effects of pregnancy, obesity and aging on the intensity of perceived breathlessness during exercise in healthy humans.* Respiratory physiology & neurobiology, 2009. **167**(1): p. 87-100.
70. O'Donnell, D.E., et al., *Mechanisms of activity-related dyspnea in pulmonary diseases.* Respiratory Physiology & Neurobiology, 2009. **167**(1): p. 116-32.
71. Casaburi, R., & Rennard, S. I., *Exercise limitation in chronic obstructive pulmonary disease. The O'Donnell threshold*, 2015. American Journal of Respiratory and Critical Care Medicine, **191**(8), 873-875.
72. Legrand, A., et al., *Respiratory effects of the scalene and sternomastoid muscles in humans.* Journal of Applied Physiology, 2003. **94**(4): p. 1467-72.
73. Mitchell, R.A., et al., *Sex differences in respiratory muscle activation patterns during high-intensity exercise in healthy humans.* Respiratory physiology & neurobiology, 2018. **247**: p. 57-60.
74. Hudson, A.L., et al., *Activation of human inspiratory muscles in an upside-down posture.* Respiratory physiology & neurobiology, 2016. **226**: p. 152-159.
75. *ATS/ERS Statement on Respiratory Muscle Testing* (2002). American Journal of Respiratory and Critical Care Medicine, **166**(4), 518-624.
76. Laveneziana, P., et al., *ERS statement on respiratory muscle testing at rest and during exercise.* Eur Respir J, 2019. **53**(6).
77. Singh, B., J.A. Panizza, and K.E. Finucane, *Diaphragm electromyogram root mean square response to hypercapnia and its intersubject and day-to-day variation.* Journal of Applied Physiology, 2005. **98**(1): p. 274-281.
78. Sinderby, C., et al., *Voluntary activation of the human diaphragm in health and disease.* Journal of Applied Physiology, 1998. **85**(6): p. 2146-2158.

79. Nguyen, D.A., et al., *Differential activation of the human costal and crural diaphragm during voluntary and involuntary breaths.* Journal of Applied Physiology, 2020. **128**(5): p. 1262-1270.
80. Hudson, A.L., et al., *Respiratory muscle activity in voluntary breathing tracking tasks: Implications for the assessment of respiratory motor control.* Respiratory physiology & neurobiology, 2020. **274**: p. 103353.
81. Luo, Y., et al., *Effect of lung volume on the oesophageal diaphragm EMG assessed by magnetic phrenic nerve stimulation.* European Respiratory Journal, 2000. **15**(6): p. 1033-1038.
82. Luo, Y., et al., *Effect of diaphragm fatigue on neural respiratory drive.* Journal of Applied Physiology, 2001. **90**(5): p. 1691-1699.
83. Ward, M., et al., *Respiratory sensation and pattern of respiratory muscle activation during diaphragm fatigue.* Journal of Applied Physiology, 1988. **65**(5): p. 2181-2189.
84. Lahrmann, H., et al., *Neural drive to the diaphragm after lung volume reduction surgery.* Chest, 1999. **116**(6): p. 1593-1600.
85. Qin, Y.Y., et al., *Effect of tiotropium on neural respiratory drive during exercise in severe COPD.* Pulmonary Pharmacology & Therapeutics, 2015. **30**: p. 51-6.
86. Jensen, D., M.R. Schaeffer, and J.A. Guenette, *Pathophysiological mechanisms of exertional breathlessness in chronic obstructive pulmonary disease and interstitial lung disease.* Current opinion in supportive and palliative care, 2018. **12**(3): p. 237-245.
87. Porszasz, J., et al., *Physiologic effects of an ambulatory ventilation system in chronic obstructive pulmonary disease.* American journal of respiratory and critical care medicine, 2013. **188**(3): p. 334-342.
88. Duiverman, M., et al., *Respiratory muscle activity and dyspnea during exercise in chronic obstructive pulmonary disease.* Respiratory physiology & neurobiology, 2009. **167**(2): p. 195-200.